

---

# A Probabilistic Framework for LLM-Based Model Discovery

---

Stefan Wahl<sup>1,2</sup> Raphaela Schenk<sup>3</sup> Ali Farnoud<sup>3</sup> Jakob H. Macke<sup>1,2,4</sup> Daniel Gedon<sup>1,2</sup>

## Abstract

Automated methods for discovering mechanistic simulator models from observational data offer a promising path toward accelerating scientific progress. Such methods often take the form of agentic-style iterative workflows that repeatedly propose and revise candidate models by imitating human discovery processes. However, existing LLM-based approaches typically implement such workflows via hand-crafted heuristic procedures, without an explicit probabilistic formulation. We recast model discovery as probabilistic inference, i.e., as sampling from an unknown distribution over mechanistic models capable of explaining the data. This perspective provides a unified way to reason about model proposal, refinement, and selection within a single inference framework. As a concrete instantiation of this view, we introduce ModelSMC, an algorithm based on Sequential Monte Carlo sampling. ModelSMC represents candidate models as particles which are iteratively proposed and refined by an LLM, and weighted using likelihood-based criteria. Experiments on real-world scientific systems illustrate that this formulation discovers models with interpretable mechanisms and improves posterior predictive checks. More broadly, this perspective provides a probabilistic lens for understanding and developing LLM-based approaches to model discovery.

## 1. Introduction

Scientific discoveries—from the expanding universe (Hubble, 1929) to gravitational waves (Abbott et al., 2016) and neuronal excitability (Hodgkin & Huxley, 1952)—often rely on formal models that integrate theory with data to en-

able interpretation and prediction. As scientific problems grow in experimental and conceptual complexity, computational simulators that encode explicit mechanistic hypotheses have become central tools for discovery (Frigg & Reiss, 2009; Winsberg, 2019; Lavin et al., 2022).

Simulators are only approximations of reality, and their fidelity depends on how accurately they capture the structure of the underlying system (Box & Draper, 1987). Constructing scientific simulators that are simultaneously interpretable, tractable, and realistic can be challenging. This modeling process requires substantial domain expertise and iterative manual refinement, rendering it labor-intensive and difficult to scale.

A range of methods have been proposed to partially automate model discovery, but existing approaches typically trade off expressive model classes against mechanistic interpretability or require substantial manual specification (Udrescu & Tegmark, 2020; Donnelly et al., 2024; Schröder & Macke, 2024). LLMs offer a qualitatively different point in this design space: trained on extensive corpora of scientific text and source code, they can generate and revise executable simulator implementations directly from textual problem formulations and feedback (Austin et al., 2021; Chen, 2021).

However, most LLM-based discovery systems are defined operationally, i.e., via prompts, agent roles, and interaction protocols, rather than as inference procedures for an explicit target distribution. As a result, these approaches (i) do not explicitly state the underlying inference problem, which hinders interpretability, obscures failure modes, and prevents principled extensions or connections to existing theory; (ii) do not naturally admit theoretical analysis or convergence properties; and (iii) rely on loosely specified agent roles and interactions, making it difficult to reason formally about the necessity or sufficiency of components.

Here, we formulate automated model discovery as a probabilistic inference problem. Given observational data  $\mathbf{x}_o$ , the goal is to sample from the unknown distribution  $p(m|\mathbf{x}_o)$  over mechanistically interpretable models  $m$  capable of explaining the data  $\mathbf{x}_o$ . Building on this formulation, we introduce ModelSMC, an approach based on Sequential Monte Carlo (SMC) methods, which approximate latent distributions using collections of weighted particles

<sup>1</sup>Machine Learning in Science, University of Tübingen, Tübingen, Germany <sup>2</sup>Tübingen AI Center, Tübingen, Germany <sup>3</sup>Boehringer Ingelheim, Biberach, Germany <sup>4</sup>Department Empirical Inference, Max Planck Institute for Intelligent Systems, Tübingen, Germany. Correspondence to: <{firstname.lastname}@uni-tuebingen.de>.

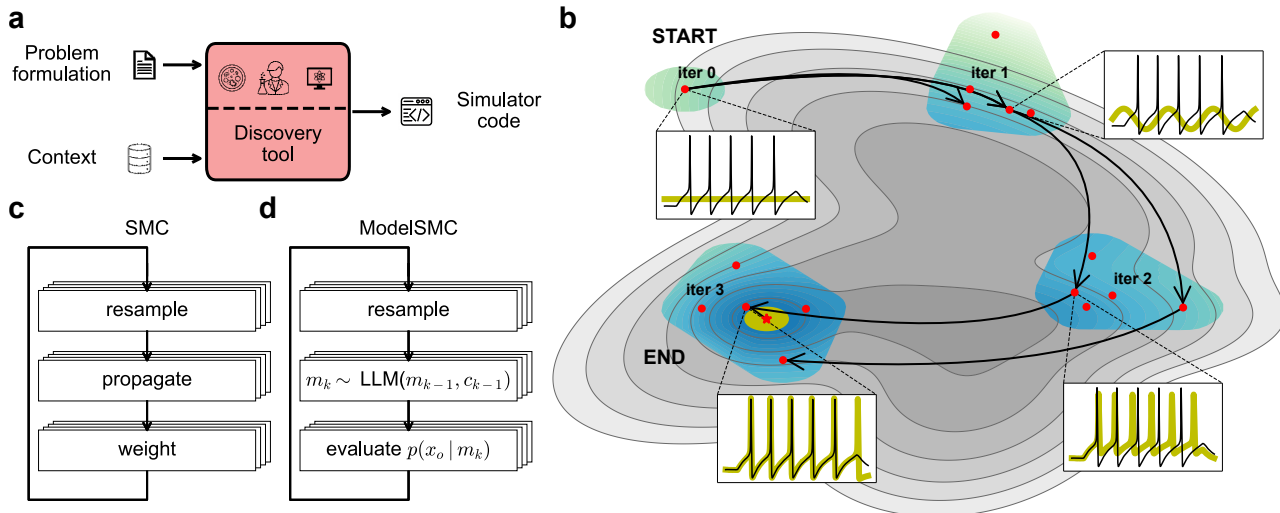


**Figure 1. Overview of ModelSMC for automated LLM-based model discovery.** (a) Given a textual problem formulation and context data, we infer a simulator model implemented in code. (b) ModelSMC iteratively refines an initial model to sample high-density regions of the model posterior  $p(m|\mathbf{x}_o)$ , approaching the unknown data-generating process (red star) in high-density regions. (c) ModelSMC is inspired by SMC, which approximates evolving distributions via weighted particles by iterative resampling, propagation, and weighting. (d) In ModelSMC, models are propagated by LLM sampling and weighted by likelihood evaluation.

(Johansen, 2009). In ModelSMC, candidate simulator models are represented as particles whose code is iteratively proposed and modified by an LLM, evaluated using likelihood-based criteria, and resampled to focus on promising (i.e., high-marginal likelihood) regions of the model space (Fig. 1).

Formulating model discovery as probabilistic inference within an SMC framework closely mirrors the iterative workflows employed by human experts, yielding conceptual and practical advantages: First, it provides an explicit mathematical formulation of the refinement process, clarifying assumptions and failure modes. Second, under standard SMC conditions, it enables principled guarantees on stability and convergence. Third, it allows formal reasoning about the role and necessity of individual system components, facilitating systematic ablations and extensions. Our main contributions can be summarized as follows:

- We cast automated LLM-based discovery of models as probabilistic inference over executable programs.
- We propose ModelSMC, an SMC-style population method with LLM-based proposals of programs.
- We demonstrate competitive performance on synthetic tasks and show that ModelSMC discovers accurate and mechanistically interpretable models on real-world neuroscience and pharmacology datasets.
- We show how existing SMC theory can be used to analyze automated model discovery with LLMs.

## 2. Related Work

**Classic mechanistic model discovery.** Automated discovery of mechanistic models has traditionally focused on symbolic regression, equation discovery, and program synthesis, including genetic programming (Schmidt & Lipson, 2009; Udrescu & Tegmark, 2020; Kamienny et al., 2022) and sparse regression over predefined libraries of candidate terms (Brunton et al., 2016; Rudy et al., 2017), as well as grammar- or DSL-based program synthesis (Gulwani et al., 2017; Parisotto et al., 2017; Ellis et al., 2021). Other approaches combine mechanistic structure with statistical learning or physics-informed models (Raissi et al., 2019; Rackauckas et al., 2020; Karniadakis et al., 2021; Donnelly et al., 2024). These methods rely on carefully engineered search spaces and have so far focused on low-complexity models. In contrast, ModelSMC explores complex simulator programs spanning hundreds of lines of code in an open search space without hand-crafted restrictions.

**LLM-based methods.** More recently, several works have used LLMs for open-ended automated model discovery. One class of approaches combines LLMs with symbolic regression or optimization loops, where the LLM proposes candidate equations or programs and iterative evaluation or gradient-based refinement is used to improve fit to data (Ma et al., 2024; Li et al., 2024; Shojaee et al., 2025; Holt et al., 2025). Another line builds on evolutionary or population-based search, exemplified by FunSearch (Romera-Paredes et al., 2024; Castro et al., 2025) or the closed-source AlphaEvolve (Novikov et al., 2025). Several works have applied these frameworks to domain-specific problems in

cognitive science (Rmus et al., 2025; Jha et al., 2025), language modeling (Cheng et al., 2025), pharmaceutical applications (Holt et al., 2024), neuroscience (Tilbury et al., 2025), or combinatorial optimization (Liu et al., 2024). Model proposal, refinement, and selection are typically defined through heuristic system designs, such as fixed agent roles, optimization loops, or evolutionary operators, rather than derived from an explicit mathematical objective.

Closest to our work are methods combining LLMs with Bayesian reasoning in scientific and probabilistic settings, such as Large Language Bayes (Domke, 2025) and AutoDiscovery (Agarwal et al., 2025). Large Language Bayes generates probabilistic programs from informal descriptions and performs approximate Bayesian inference via likelihood-weighted model averaging. AutoDiscovery explores nested hypotheses using Bayesian surprise within a Monte Carlo tree search, without explicitly defining a posterior over mechanistic models or maintaining a population of executable models. In contrast, we frame mechanistic model discovery as inference over models  $p(m|x_o)$ .

**Probabilistic model inference.** Probabilistic approaches to model discovery and comparison are traditionally grounded in Bayesian model selection and averaging, where candidate models are evaluated via marginal likelihoods or Bayes factors (Kass & Raftery, 1995; Morey et al., 2016), as well as Bayesian program induction (Lake et al., 2015). With simulators as tools for scientific inquiry, this has motivated simulation-based and likelihood-free inference methods, including synthetic likelihoods and neural density estimation (Cranmer et al., 2020; Deistler et al., 2025). It also includes SMC samplers for static or trans-dimensional targets, where explicit likelihood tempering bridges from prior to posterior to mitigate weight degeneracy (Del Moral et al., 2006; Neal, 2001). Recent work, such as simulation-based model inference (Schröder & Macke, 2024), extends this view to simultaneous model and parameter inference over graph-structured components using amortized inference, but assumes a fixed compositional prior without iterative refinement. In contrast, ModelSMC treats full model programs as latent variables and uses LLMs as proposals for open-ended model spaces, progressively concentrating on high-likelihood regions without an explicit tempering schedule.

## 3. Method

### 3.1. Background: Sequential Monte Carlo

SMC methods (Johansen, 2009; Naesseth et al., 2019) approximate a sequence of target probability distributions using a set of weighted samples. Consider a state space model with latent states  $x_{1:T}$  and observations  $y_{1:T}$ , with joint density  $p(x_{1:T}, y_{1:T})$ . The inference task is to approxi-

mate the filtering or target distribution  $p(x_t|y_{1:t})$ . At each time step  $t$ , SMC represents the distribution using a finite set of  $N$  particles  $\{x_t^i\}_{i=1}^N$  and associated weights  $\{w_t^i\}_{i=1}^N$  that together define an empirical measure

$$p(x_t|y_{1:t}) \approx \sum_{i=1}^N w_t^i \delta_{x_t^i}, \quad (1)$$

providing a discrete approximation of the target distribution. In practice  $N$  is of the order  $10^2$ – $10^5$ . Convergence results guarantee that, under mild conditions, the particle approximation converges to the true target distribution as  $N \rightarrow \infty$  (Del Moral, 2004; Johansen, 2009).

As a specific instantiation of SMC, we consider the bootstrap particle filter. Given particles at time  $t-1$ , the update at time  $t$  consists of the following steps:

1. **Resample.** Sample ancestor indices  $a_t^i \sim \mathcal{C}(\{w_{t-1}^j\}_{j=1}^N)$ , where  $\mathcal{C}$  denotes the categorical distribution.
2. **Propagate.** Sample new particles from the transition model,  $x_t^i \sim p(x_t|x_{t-1}^{a_t^i})$ .
3. **Weight.** Assign unnormalized weights using the likelihood,  $\tilde{w}_t^i = p(y_t|x_t^i)$  and normalize  $w_t^i = \frac{\tilde{w}_t^i}{\sum_{j=1}^N \tilde{w}_t^j}$ .

Repeating these steps sequentially for  $t = 1, \dots, T$  yields a particle-based approximation of the target distributions. SMC can also be used when the target distribution is static, i.e.,  $p(x_t) \equiv p(x)$  for all  $t$ , by defining an artificial sequence of intermediate target distributions that progressively transform a simple initial distribution into the desired target (e.g., via likelihood tempering) (Neal, 2001; Del Moral et al., 2006).

### 3.2. Problem Formulation

Scientific model discovery aims to infer a model  $m$  that reproduces the observable behavior of a system of interest  $m^*$ . Information about  $m^*$  is available only through an observed set  $x_o = \{(x_o^j, c_o^j)\}_{j=1}^M$ , where each observation  $x_o^j$  is generated by  $m^*$  under context  $c_o^j$ . The context may include, e.g., initial conditions or experimental parameters. We assume the observed data pairs are iid.

A model  $m$  is an algorithm written in code that probabilistically maps context  $c \in \mathcal{C}$  and model parameters  $\theta \in \Theta$  to data  $x \in \mathcal{X}$ . The model parameters  $\theta$  are not assumed to be known but fall within a prior distribution  $p(\theta)$ . For notational simplicity, we abbreviate  $m(c, \theta) \equiv m$ .

From a probabilistic perspective, model discovery corresponds to inference over models conditioned on the observed data. The inference target is a distribution over

models  $p(m|\mathbf{x}_o)$  that assigns higher probability to models whose simulated behavior matches the observed behavior of  $m^*$  across contexts. This distribution is defined implicitly via a likelihood and a prior: the likelihood  $p(x_o|m)$  is induced by executing the simulator model defined by  $m$  with latent parameters  $\theta \sim p(\theta)$ . The prior  $p(m)$  corresponds to the marginal distribution over model implementations induced by an LLM-based generative process. The distribution  $p(m|\mathbf{x}_o)$  is generally intractable due to model space size and the absence of an explicit likelihood.

### 3.3. SMC-Based Model Discovery with ModelSMC

ModelSMC approximates the posterior  $p(m|\mathbf{x}_o)$  using a population of candidate models that is iteratively refined using SMC (see Sec. 3.1). Since the underlying system  $m^*$  is fixed, the SMC time index corresponds to iterative refinement rather than temporal evolution. Unlike classical SMC, each particle corresponds to a candidate model rather than a dynamical state.

Each particle represents a candidate model and is associated with a weight reflecting its posterior relevance. In addition to the model implementation, particles store auxiliary context such as evaluation feedback. A particle consists of the tuple of model, weight and context  $(m^i, w^i, c^i)$  for  $i = 1, \dots, N$  particles.

ModelSMC proceeds for  $K$  iterations. In each iteration  $k$ , particles are resampled according to their weight, propagated to generate new candidate models, and weighted according to their likelihood under the observed data. Each iteration consists of three steps: (i) resampling, (ii) propagation, and (iii) weighting. Algorithm 1 summarizes the complete procedure.

**Resampling.**  $N$  particles are resampled according to their normalized weights. Each new particle is associated with an ancestor index  $a$ , determining the particles used in the propagation step (Eq. 2).

**Propagation.** Each resampled particle is propagated via a mixture kernel (Eq. 3). With probability  $\alpha$ , the particle is cloned unchanged, and with probability  $1 - \alpha$ , the LLM samples a model implementation conditioned on (i) the models along its ancestry, (ii) their associated contextual feedback, and (iii) a fixed task-specific prompt  $c_{\text{task}}$  encoding domain knowledge, implementation constraints, and evaluation criteria.

The context  $c_{k-1}^a$  summarizes the recent ancestry of the particle and its performance and is generated via an auxiliary LLM call based on the particle’s weight. To control computational cost and prompt length, only a limited number of the most recent ancestry elements are included. The probability  $\alpha$  controls the trade-off between exploration and exploitation: cloned particles require no new

---

#### Algorithm 1 ModelSMC (for $i = 1, \dots, N$ )

---

**Input:** Number of particles  $N$ , number of iterations  $K$ , cloning probability  $\alpha \in [0, 1]$ , observed data  $\mathbf{x}_o = \{(x_o^j, c_o^j)\}_{j=1}^M$ , task prompt  $c_{\text{task}}$ , initial particle and weight  $(m_0, w_0 = 1)$ .

- 1: **for**  $k = 1, \dots, K$  **do**
- 2:    $\triangleright$  **1. Resample**
- 3:   Sample ancestor indices

$$a_k^i \sim \text{Cat}(\{w_{k-1}^j\}_{j=1}^N), \quad i = 1, \dots, N. \quad (2)$$

- 4:    $\triangleright$  **2. Propagate**
- 5:   Propagate each particle  $m_k^i$  for  $i = 1, \dots, N$  by first sampling  $z \sim \mathcal{U}[0, 1]$ , then

$$m_k^i \sim \begin{cases} \delta_{m_{k-1}^{a_k^i}}, & \text{if } z < \alpha, \\ p_{\text{LLM}}(m \mid m_{k-1}^{a_k^i}, c_{k-1}^{a_k^i}, c_{\text{task}}), & \text{else.} \end{cases} \quad (3)$$

- 6:    $\triangleright$  **3. Weight**
- 7:   Get surrogate likelihood  $p_\phi(x \mid m_k^i, \theta, c)$ .
- 8:   Compute marginal likelihood for each  $(x_o^j, c_o^j) \in \mathbf{x}_o$

$$p(x_o^j \mid m_k^i) = \int p(\theta) p_\phi(x_o^j \mid m_k^i, \theta, c_o^j) d\theta. \quad (4)$$

- 9:   Update weights  $\tilde{w}_k^i$  and normalize to obtain  $w_k^i$

$$\tilde{w}_k^i = \left( \prod_{j=1}^M p(x_o^j \mid m_k^i) \right)^{1/M}. \quad (5)$$

- 10:   Generate feedback  $c_k^i = \text{LLM}(m_k^i, w_k^i)$ .
- 11: **end for**

**Output:** Particles and weights  $\{m_K^i, w_K^i\}_{i=1}^N$ .

---

simulations or likelihood evaluations, preserving computational resources, while newly proposed particles explore the model space. Selection among clones is handled implicitly by resampling based on likelihood weights.

This iterative adaptation of the proposal plays a role analogous to likelihood tempering in classical SMC samplers (Del Moral et al., 2006): early iterations explore the model space broadly, while later iterations concentrate proposals around high-likelihood candidates as ancestry and feedback accumulate. Unlike explicit tempering, this annealing occurs in the proposal distribution rather than the target, and without formal variance-control guarantees.

**Weighting.** Each generated model  $m^i$  is assigned a weight proportional to the likelihood of the observed data,

$$\tilde{w}_k^i = p(x_o \mid m_k^i). \quad (6)$$

Assuming iid observed data, the likelihood factorizes across samples. For improved numerical stability, we use a normalized geometric mean (Eq. 5). Weighting models by likelihood is consistent with the posterior  $p(m|\mathbf{x}_o)$  as target (under idealized assumptions; derivation in Sec. B).

The likelihood  $p(x_o|m^i)$  induced by a model is generally intractable. To obtain an estimate of the likelihood, we can sample from the likelihood by evaluating the model at different values of  $(\theta, c)$ . Specifically, we sample a synthetic dataset  $\theta \sim p(\theta)$ ,  $c \sim p(c)$ ,  $x \sim p(x|m^i(\theta, c))$  and train a conditional density estimator  $p_\phi(x|m^i, \theta, c)$ . This approach is also known as Neural Likelihood Estimation (Papamakarios et al., 2019, NLE). Given a trained likelihood surrogate, the marginal likelihood for each observed data instance is obtained by integrating out  $\theta$  via Monte Carlo approximation (Eq. 4). We note that the trained likelihood estimation is an approximation of the true likelihood (details in Sec. D.2).

For NLE, we adapt a likelihood-estimation variant derived from NPE-PFN (Vetter et al., 2025). This approach uses the pretrained tabular foundation model TabPFN as a density estimator, enabling training-free likelihood estimation (Hollmann et al., 2025). Crucially, this eliminates the need for a separate likelihood estimation training loop at each iteration of ModelSMC, which is especially beneficial in model discovery where repeated likelihood evaluations are required. The foundation model is particularly efficient with small simulation budgets. Our likelihood estimation approach allows ModelSMC to generate non-differentiable models without any explicit parameter optimization.

**Implementation Remarks.** Simulating and evaluating new models is computationally expensive; cloned particles avoid this cost entirely, which motivates the mixture kernel in Eq. 3. In the current implementation, the two branches use slightly different resampling: cloned particles are selected *without replacement* from the weighted pool to maintain diversity among retained models, while ancestor indices for LLM propagation are sampled *with replacement*, allowing multiple proposals to originate from the highest-weight model. This deviation from the idealized algorithm, chosen for computational convenience, does not affect the weighting step or the theoretical properties of the algorithm.

ModelSMC differs from prior model discovery methods in two key aspects. First, the weighting step is derived from the model posterior  $p(m|x_o)$ , providing a principled probabilistic objective rather than relying on alternative discrepancy measures such as MMD, MSE, or Wasserstein distance (Gretton et al., 2012; Arjovsky et al., 2017). Second, ModelSMC marginalizes over model parameters  $\theta$  during discovery instead of optimizing point estimates, thereby reducing sensitivity to parameter uncertainty. For downstream use of discovered models, we perform parameter inference using neural posterior estimation (NPE) (Lueckmann et al., 2017; Papamakarios & Murray, 2016) and NPE-PFN (Vetter et al., 2025) (details in Sec. D.1).

### 3.4. Theoretical Insights

Since our framework is based on SMC, we connect ModelSMC to classical SMC theory and show that, under mild assumptions on the LLM-based propagation mechanism, ModelSMC provides a consistent Monte Carlo approximation of the model posterior  $p(m|x_o)$  (Chopin, 2004; Del Moral, 2004). This establishes a formal connection framing LLM-driven automated model discovery as asymptotically consistent Bayesian inference over models.

**Theorem 3.1** (Consistency of ModelSMC). *Let  $\pi(m) \propto p(x_o|m)p(m)$  be a fixed target distribution over models, and let  $q(m'|m)$  denote an idealized proposal kernel induced by the propagation step. Assume (i) support coverage, i.e., any  $m$  with  $\pi(m) > 0$  can be generated with non-zero probability; (ii) uniformly bounded importance weights; (iii) conditional independence of propagated particles given resampling; and (iv) exact likelihood evaluation, i.e., the importance weights are computed using the true marginal likelihood  $p(x_o|m)$ . Let  $\{(m^i, w^i)\}_{i=1}^N$  be the particle population at a fixed iteration. Then, for any bounded test function  $\varphi$ ,*

$$\sum_{i=1}^N w^i \varphi(m^i) \xrightarrow{\mathbb{P}} \mathbb{E}_\pi[\varphi(m)] \quad \text{as } N \rightarrow \infty, \quad (7)$$

with asymptotic variance  $\mathcal{O}(1/N)$ . The result holds in the presence of resampling.

The proof is provided in Sec. C. Theorem 3.1 implies that, under idealized assumptions, ModelSMC is statistically consistent: the algorithm is asymptotically unbiased and its particles approximate  $p(m|x_o)$ . This provides a principled foundation for LLM-based automated model discovery.

## 4. Experiments

### 4.1. Validation of ModelSMC for Model Discovery

We first validate the core probabilistic inference mechanism underlying ModelSMC in a controlled setting where the ground-truth model is known, and the model proposal is not affected by the LLM. We consider an LLM-free variant of ModelSMC on a finite model space with 20 candidates. Each candidate is a 10-dimensional Gaussian mixture models with varying numbers of components and dense covariances (details in Sec. F.1). In this setting, the propagation step reduces to copying resampled particles, and no text-based feedback is used. Observational data are drawn from one of the 20 models.

Across all runs, the particle population rapidly concentrates on the ground-truth model, despite weighting particles using an approximate likelihood estimate  $p_\phi(x_o|m)$ . Specifically, after a small number of iterations, resampling selects the true model with probability approaching one (Fig. 2).

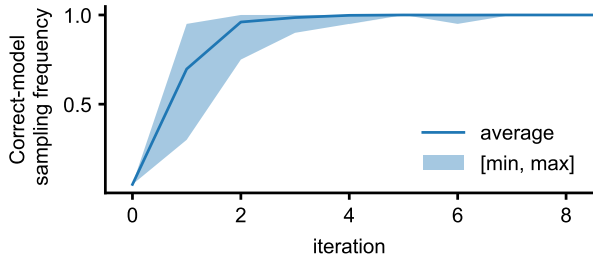


**Figure 2. Relative sampling frequency of the target model for LLM-free ModelSMC.** Sampling frequencies averaged over ten different target models and ten experiments each. Shaded region: The highest and the lowest sampling frequency observed at each time step over all runs.

**Table 1. Performance evaluation.** We evaluate the median metrics for the best particles over ten discovery runs. Results including confidence intervals are reported in Appendix Table G-1.

	ModelSMC	$-\frac{1}{M} \log p(x_o m)(\downarrow)$ FunSearch+	ModelSMC $N=1$
SIR	<b>-503.37</b>	-500.00	-464.17
Kidney	<b>43.58</b>	N/A	46.29
HH	<b>25.18</b>	28.96	25.95
		$-\frac{1}{M} \log p(x_o \hat{\theta}, m)(\downarrow)$	
SIR	<b>-492.67</b>	-492.05	-455.13
Kidney	<b>55.05</b>	N/A	58.63
HH	15.47	<b>12.05</b>	15.64

This behavior is consistent across ground-truth choices and random seeds.

This experiment isolates the inference component of ModelSMC and shows that, in a finite model space, the algorithm concentrates posterior mass on the true data-generating process, behaving as a consistent posterior sampler over models. Thus, once the ground-truth model is proposed by the LLM, ModelSMC reliably identifies it. These results verify the inference procedure of ModelSMC.

## 4.2. Quantitative Results

We perform a quantitative evaluation of ModelSMC across three model discovery tasks: a synthetic epidemiological system with known ground-truth dynamics (SIR; Sec. F.2), a pharmacological simulator of kidney aldosterone regulation implemented in R (Sec. 4.3), and a neuroscience Hodgkin-Huxley (HH) neuron simulator (Sec. 4.4). ModelSMC targets model discovery as mechanistic equations for complex simulator models. We therefore compare against two baselines matching this scope: (i) a modified FunSearch (Romera-Paredes et al., 2024) that optimizes free model parameters and uses likelihood-based weights (Castro et al., 2025), and (ii) ModelSMC with a single par-

ticle ( $N=1$ ), which removes the population-based inference of the full algorithm. FunSearch+ is Python-specific, which prevents direct application to the R-based kidney simulator. We do not compare with classical symbolic regression because it is typically limited to low-complexity functions (Schmidt & Lipson, 2009), and black-box predictive models, such as transformers, because they lack mechanistic interpretability.

Across all tasks, ModelSMC achieves strong quantitative performance (Table 1). On both synthetic and real-world tasks, it attains high marginal and conditional likelihoods, matching at least the baseline performance at comparable computational budgets (Appendix Fig. G-1). Unlike FunSearch+, ModelSMC handles any coding language.

These results indicate that framing model discovery as an inference problem does not compromise quantitative performance. Instead, ModelSMC discovers competitive mechanistic models while providing the probabilistic foundation that enables additional interpretability and analysis.

## 4.3. Pharmacological Kidney Model

We evaluate ModelSMC on a real-world quantitative systems pharmacology (QSP) problem. Specifically, we adapt a simulator model of plasma potassium regulation in the kidney mediated by aldosterone, a key steroid hormone (Maddah & Hallow, 2022). The original model is implemented in R using RxODE2 (Wang et al., 2016; R Core Team, 2025) and is derived from first principles of pharmacokinetics and pharmacodynamics, capturing renal excretion, tubular reabsorption, and hormonal feedback. In the model, the aldosterone mechanism is empirically fitted rather than biophysically derived (Maddah & Hallow, 2022).

In this experiment, we intentionally replace the aldosterone mechanism with a constant term (Fig. 3(a), left), thereby introducing a targeted structural misspecification. ModelSMC is tasked with inferring the missing regulatory dynamics from the data. The inference problem is particularly challenging due to extremely limited data: four patient intake scenarios (high/low K  $\times$  high/low Na), with a single measurement of plasma potassium and aldosterone at five time points per scenario (Dluhy et al., 1972). Experimental details are provided in Sec. F.3.

Across all seeds, ModelSMC assigns high posterior weight to a narrow family of aldosterone feedback mechanisms whose functional form closely matches the originally proposed model (Fig. 3(a), right, for one model). Although individual particles differ in structural details, models encoding qualitatively different regulatory hypotheses receive negligible posterior weight. Posterior predictive simulations from high-probability models closely track observed

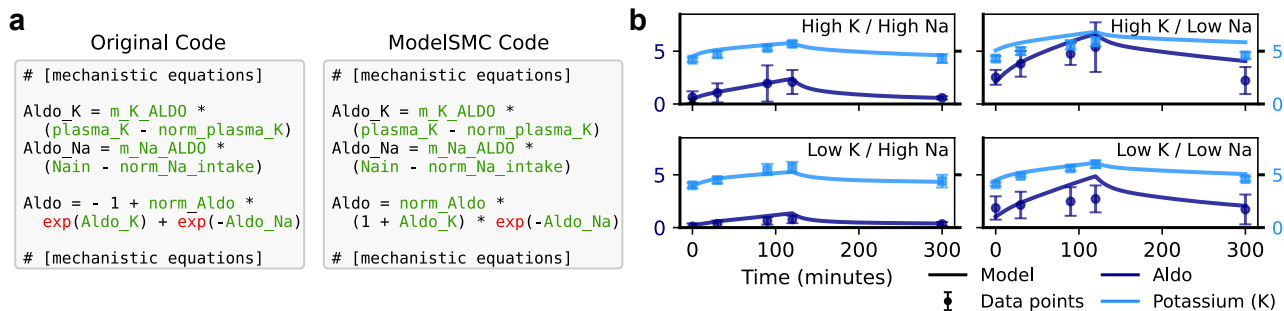


Figure 3. **Systems pharmacology kidney model with experimental data.** (a) Original code snippet in R for the aldosterone mechanism (left) and one instance of the inferred model code (right). (b) Posterior predictive for the code instance in (a) with real-world data points.

plasma potassium and aldosterone measurements, despite the limited data (Fig. 3(b)).

From an inference perspective, this experiment illustrates strong posterior concentration over a mechanistically coherent class rather than the selection of a single best-fitting model. The absence of competing high-weight alternatives indicates that the available data are sufficient to rule out broad classes of hypotheses, indicating that the data suffice to diagnose structural inadequacy rather than parameter uncertainty. Compared to methods producing a single point estimate, ModelSMC yields a posterior over low-complexity mechanisms that both generalize in posterior predictive checks and quantify uncertainty over plausible mechanisms.

#### 4.4. Hodgkin-Huxley Model

Finally, we evaluate ModelSMC on a neuroscience simulator model of neuronal membrane dynamics. Specifically, we consider the single-compartment Hodgkin-Huxley (HH) model of action potential generation (Hodgkin & Huxley, 1952; Pospischil et al., 2008), which describes membrane voltage dynamics via nonlinear ion-channel conductances and gating variables. As a baseline, we consider the same simulator from Gonçalves et al. (2020), consisting of eight biophysical parameters and explicit ion channels for sodium, potassium, and leak current. While this model provides a strong description of neuronal dynamics, it can exhibit systematic discrepancies when fitted to real recordings (Gao et al., 2023; Bernaerts et al., 2025). Observations consist of membrane voltage traces summarized by seven standard summary statistics (Gonçalves et al., 2020). We consider 10 real voltage recordings from the Allen Cell Types Database (Allen Institute for Brain Science, 2015).

In contrast to prior work focusing exclusively on parameter inference (Gonçalves et al., 2020; Vetter et al., 2025), we treat the HH model as a structural inference problem. Taking the baseline HH model, ModelSMC is tasked with

inferring additional ion-channel mechanisms that improve model specification and reduce systematic mismatch to data. This setting is particularly challenging due to the limited number of real-world observations, the already high fidelity of the baseline model, and the need to detect subtle but consequential structural deficiencies rather than gross misspecification. For experimental conditions, see Sec. F.4.

ModelSMC shows rapid posterior concentration while continuing to explore multiple high-likelihood structural variants over successive iterations (Fig. 4(a)). For a representative run, particle ancestry reveals a diverse sampling of the model space with distinct ion-channel extensions of the baseline HH model (Fig. 4(a) opaque). Across runs, high posterior weight is consistently assigned to models introducing additional slow potassium or persistent sodium currents, including M-type, A-type, and  $\text{Na}_P$  channels. Within these families, refinements such as voltage-dependent activation time constants receive increased posterior weight and improve posterior predictive agreement with recorded voltage traces, particularly for spike-frequency adaptation (Fig. 4 b,c).

Rather than identifying a single revised HH model, ModelSMC yields a posterior over mechanistically interpretable extensions, with comparable explanatory power. The posterior exposes residual non-identifiability in ion-channel composition while isolating robust conclusions, i.e., the extension with additional slow currents. Thus, posterior mass serves as a diagnostic: low-weight regions indicate genuine structural mismatch, while clusters of high-probability models reveal symmetries and ambiguities that are invisible to single-model discovery.

## 5. Discussion

We formulated automated discovery of mechanistic models as Bayesian inference over programs. We introduced ModelSMC, an SMC-based algorithm that uses LLMs as proposal distributions. Unlike prior agentic systems, ModelSMC directly approximates the posterior  $p(m|x_o)$  by

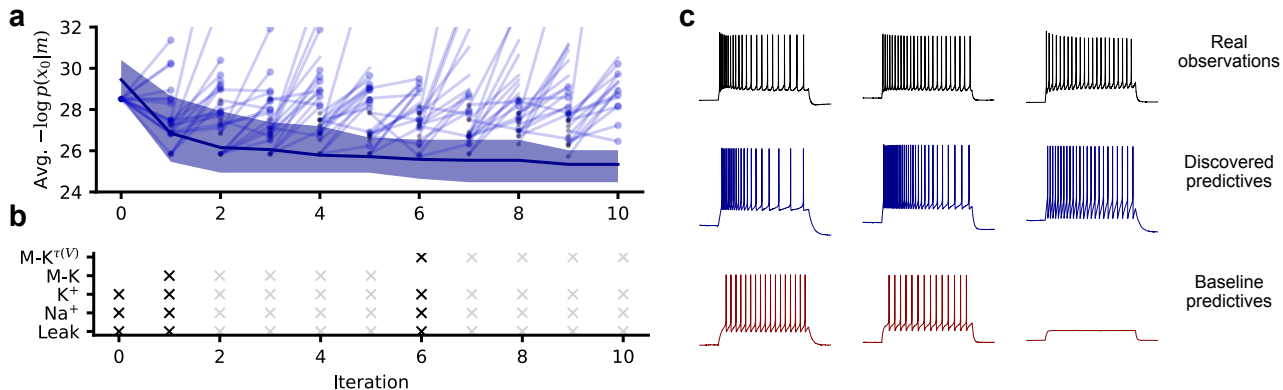


**Figure 4. Hodgkin-Huxley model with Allen cell types database data.** Results are shown for one representative random seed from the 10 runs, used consistently across panels. **(a)** ModelSMC convergence across runs, showing the mean (solid line) and 95% percentiles (shaded). With lower opacity, we overlay the full model ancestry of the selected run. **(b)** For the selected run, highlighting of inferred ion-channel mechanisms at successive improvement stages. **(c)** Posterior predictive voltage simulations for real observations from the Allen database, comparing the baseline HH model to the best model identified in the selected run.

marginalizing over parameters. This approach produces a weighted population of models, revealing which hypotheses concentrate posterior mass, which remain uncertain, and which are non-identifiable. Across synthetic and real-world systems, this enables diagnosing which mechanistic hypotheses are strongly supported, ruled out, or remain as plausible alternatives under limited data.

A natural question is whether automated discovery systems generate genuinely novel scientific insights or primarily re-discover known mechanisms. We emphasize that our primary contribution is methodological: we introduce a general inference framework in which such questions can be meaningfully posed. Whether novel mechanisms emerge depends on the application, data, and modeling assumptions, and is orthogonal to the validity of the inference framework itself. Practically, ModelSMC applies to settings where candidate models can be executed and admit reliable likelihood approximation. In such domains, probabilistic reasoning over models is well-defined and informative.

**Limitations.** We introduce an inference framework for model discovery, instantiated by ModelSMC. Limitations arise at algorithmic and framework levels: First, ModelSMC is computationally expensive due to repeated simulation and likelihood estimation for each candidate model. This could be alleviated by multi-fidelity simulation, adaptive particle budgets, or early-rejection strategies from SMC literature. Second, posterior weights rely on surrogate likelihoods, which may introduce bias under misspecification. Incorporating uncertainty-aware or robust likelihood estimation is an important direction. Third, the discovery process is bottlenecked by the LLM’s ability to propose relevant model structures. Improvements in foundation models, domain-specific pretraining, or retrieval-

augmented generation will directly enhance discovery performance (Lewis et al., 2020). Finally, while posterior weights provide a principled clustering and ranking, models remain high-dimensional programs without an explicit geometry. Developing notions of similarity or clustering over model space would enable richer posterior analysis and enhance inference with semantic structure over program spaces.

**Conclusion.** By reframing LLM-driven model discovery as probabilistic inference, we provide a framework that unifies proposal, refinement, and selection under a single probabilistic objective. ModelSMC provides one concrete instantiation of this view, combining LLM-based proposals with likelihood-based weighting to approximate a posterior over mechanistic models. Crucially, this connection enables direct use of established Monte Carlo methodology, including particle rejuvenation moves (Gordon et al., 1993), SMC samplers for static targets (Del Moral et al., 2006), adaptive resampling schemes (Doucet et al., 2001; Johansen, 2009; Del Moral et al., 2012), and annealed or tempered objectives (Neal, 2001). More broadly, this perspective situates recent LLM-based discovery systems within a well-studied inference framework, providing a common language for comparison, analysis, and systematic development of future methods.

## Acknowledgements

We thank Manuel Gloeckler for feedback on the manuscript, members of the Mackelab for discussions, and Julian Schwab for domain expertise on the QSP experiment. This work was funded by the German Research Foundation (DFG) under Germany’s Excellence Strategy – EXC number 2064/1 – 390727645 and SFB 1233 ‘Robust

Vision’ (276693517), and the Boehringer Ingelheim AI & Data Science Fellowship Program. SW is a member of the International Max Planck Research School for Intelligent Systems (IMPRS-IS).

## Impact Statement

This paper presents work whose goal is to advance the field of Machine Learning. There are many potential societal consequences of our work, none of which we feel must be specifically highlighted here.

## References

- Abbott, B. P., Abbott, R., Abbott, T. D., Abernathy, M. R., Acernese, F., Ackley, K., Adams, C., Adams, T., Addesso, P., Adhikari, R. X., et al. Observation of gravitational waves from a binary black hole merger. *Physical review letters*, 116(6):061102, 2016.
- Agarwal, D., Majumder, B. P., Adamson, R., Chakravorty, M., Gavireddy, S. R., Parashar, A., Surana, H., Mishra, B. D., McCallum, A., Sabharwal, A., and Clark, P. AutoDiscovery: Open-ended scientific discovery via Bayesian surprise. In *The Thirty-ninth Annual Conference on Neural Information Processing Systems*, 2025.
- Allen Institute for Brain Science. Allen cell types database. <https://celltypes.brain-map.org>, 2015.
- Arjovsky, M., Chintala, S., and Bottou, L. Wasserstein generative adversarial networks. In *International conference on machine learning*, pp. 214–223, 2017.
- Austin, J., Odena, A., Nye, M., Bosma, M., Michalewski, H., Dohan, D., Jiang, E., Cai, C., Terry, M., Le, Q., et al. Program synthesis with large language models. *arXiv preprint arXiv:2108.07732*, 2021.
- Bernaerts, Y., Deistler, M., Gonçalves, P. J., Beck, J., Stimberg, M., Scala, F., Tolia, A. S., Macke, J. H., Kobak, D., and Berens, P. Combined statistical-biophysical modeling links ion channel genes to physiology of cortical neuron types. *Patterns*, 6(10), 2025.
- Boelts, J., Deistler, M., Gloeckler, M., Álvaro Tejero-Cantero, Lueckmann, J.-M., Moss, G., Steinbach, P., Moreau, T., Muratore, F., Linhart, J., Durkan, C., Vetter, J., Miller, B. K., Herold, M., Ziaemehr, A., Pals, M., Gruner, T., Bischoff, S., Krouglova, N., Gao, R., Lappalainen, J. K., Mucsányi, B., Pei, F., Schulz, A., Stefanidi, Z., Rodrigues, P., Schröder, C., Zaid, F. A., Beck, J., Kapoor, J., Greenberg, D. S., Gonçalves, P. J., and Macke, J. H. sbi reloaded: a toolkit for simulation-based inference workflows. *Journal of Open Source Software*, 10(108):7754, 2025.
- Box, G. E. and Draper, N. R. *Empirical model-building and response surfaces*. John Wiley & Sons, 1987.
- Brunton, S. L., Proctor, J. L., and Kutz, J. N. Discovering governing equations from data by sparse identification of nonlinear dynamical systems. *Proceedings of the National Academy of Sciences*, 113(15):3932–3937, 2016.
- Castro, P. S., Tomasev, N., Anand, A., Sharma, N., Mohanta, R., Dev, A., Perlin, K., Jain, S., Levin, K., Elteto, N., Dabney, W., Novikov, A., Turner, G. C., Eckstein, M. K., Daw, N. D., Miller, K. J., and Stachenfeld, K. Discovering symbolic cognitive models from human and animal behavior. In *Forty-second International Conference on Machine Learning*, 2025.
- Chen, M. Evaluating large language models trained on code. *arXiv preprint arXiv:2107.03374*, 2021.
- Cheng, J., Clark, P., and Richardson, K. Language modeling by language models. In *The Thirty-ninth Annual Conference on Neural Information Processing Systems*, 2025.
- Chopin, N. Central limit theorem for sequential Monte Carlo methods and its application to Bayesian inference. 2004.
- Cranmer, K., Brehmer, J., and Louppe, G. The frontier of simulation-based inference. *Proceedings of the National Academy of Sciences*, 117(48):30055–30062, 2020.
- Deistler, M., Boelts, J., Steinbach, P., Moss, G., Moreau, T., Gloeckler, M., Rodrigues, P. L., Linhart, J., Lappalainen, J. K., Miller, B. K., et al. Simulation-based inference: A practical guide. *arXiv preprint arXiv:2508.12939*, 2025.
- Del Moral, P. *Feynman-Kac formulae: genealogical and interacting particle systems with applications*. Springer, 2004.
- Del Moral, P., Doucet, A., and Jasra, A. Sequential monte carlo samplers. *Journal of the Royal Statistical Society Series B: Statistical Methodology*, 68(3):411–436, 2006.
- Del Moral, P., Doucet, A., and Jasra, A. An adaptive sequential Monte Carlo method for approximate Bayesian computation. *Statistics and computing*, 22(5):1009–1020, 2012.
- Dluhy, R. G., Axelrod, L., Underwood, R. H., Williams, G. H., et al. Studies of the control of plasma aldosterone concentration in normal man: II. effect of dietary potassium and acute potassium infusion. *The Journal of clinical investigation*, 51(8):1950–1957, 1972.
- Domke, J. Large Language Bayes. In *The Thirty-ninth Annual Conference on Neural Information Processing Systems*, 2025.

- Donnelly, J., Daneshkhah, A., and Abolfathi, S. Physics-informed neural networks as surrogate models of hydrodynamic simulators. *Science of The Total Environment*, 912:168814, 2024.
- Doucet, A., De Freitas, N., Gordon, N. J., et al. *Sequential Monte Carlo methods in practice*, volume 1. 2001.
- Ellis, K., Wong, C., Nye, M., Sablé-Meyer, M., Morales, L., Hewitt, L., Cary, L., Solar-Lezama, A., and Tenenbaum, J. B. Dreamcoder: Bootstrapping inductive program synthesis with wake-sleep library learning. In *Proceedings of the 42nd acm sigplan international conference on programming language design and implementation*, pp. 835–850, 2021.
- Frigg, R. and Reiss, J. The philosophy of simulation: hot new issues or same old stew? *Synthese*, 169(3):593–613, 2009.
- Gao, R., Deistler, M., and Macke, J. H. Generalized Bayesian inference for scientific simulators via amortized cost estimation. *Advances in Neural Information Processing Systems*, 36:80191–80219, 2023.
- Gonçalves, P. J., Lueckmann, J.-M., Deistler, M., Nonnenmacher, M., Öcal, K., Bassetto, G., Chintaluri, C., Podlaski, W. F., Haddad, S. A., Vogels, T. P., et al. Training deep neural density estimators to identify mechanistic models of neural dynamics. *Elife*, 9:e56261, 2020.
- Gordon, N. J., Salmond, D. J., and Smith, A. F. Novel approach to nonlinear/non-Gaussian Bayesian state estimation. In *IEE proceedings F (radar and signal processing)*, volume 140, pp. 107–113, 1993.
- Gretton, A., Borgwardt, K. M., Rasch, M. J., Schölkopf, B., and Smola, A. A kernel two-sample test. *The journal of machine learning research*, 13(1):723–773, 2012.
- Gulwani, S., Polozov, O., and Singh, R. Program synthesis. *Foundations and trends in programming languages*, 4(1-2):1–119, 2017.
- Harris, C. R., Millman, K. J., van der Walt, S. J., Gommers, R., Virtanen, P., Cournapeau, D., Wieser, E., Taylor, J., Berg, S., Smith, N. J., Kern, R., Picus, M., Hoyer, S., van Kerkwijk, M. H., Brett, M., Haldane, A., del Río, J. F., Wiebe, M., Peterson, P., Gérard-Marchant, P., Sheppard, K., Reddy, T., Weckesser, W., Abbasi, H., Gohlke, C., and Oliphant, T. E. Array programming with NumPy. *Nature*, 585(7825):357–362, 2020.
- Hodgkin, A. L. and Huxley, A. F. A quantitative description of membrane current and its application to conduction and excitation in nerve. *J Physiol*, 117(4):500–544, 1952.
- Hollmann, N., Müller, S., Purucker, L., Krishnakumar, A., Körfer, M., Hoo, S. B., Schirrmeister, R. T., and Hutter, F. Accurate predictions on small data with a tabular foundation model. *Nature*, 01 2025.
- Holt, S., Qian, Z., Liu, T., Weatherall, J., and van der Schaar, M. Data-driven discovery of dynamical systems in pharmacology using large language models. *Advances in Neural Information Processing Systems*, 37:96325–96366, 2024.
- Holt, S., Luyten, M. R., Berthon, A., and van der Schaar, M. G-Sim: Generative simulations with large language models and gradient-free calibration. In *Forty-second International Conference on Machine Learning*, 2025.
- Hubble, E. A relation between distance and radial velocity among extra-galactic nebulae. *Proceedings of the national academy of sciences*, 15(3):168–173, 1929.
- Hunter, J. D. Matplotlib: A 2d graphics environment. *Computing in Science & Engineering*, 9(3):90–95, 2007.
- Jha, K., Huang, A. Y., Ye, E., Jaques, N., and Kleiman-Weiner, M. Modeling others’ minds as code. *arXiv preprint arXiv:2510.01272*, 2025.
- Johansen, A. A tutorial on particle filtering and smoothing: Fifteen years later. 2009.
- Kamienny, P.-A., d’Ascoli, S., Lample, G., and Charton, F. End-to-end symbolic regression with transformers. *Advances in Neural Information Processing Systems*, 35:10269–10281, 2022.
- Karniadakis, G. E., Kevrekidis, I. G., Lu, L., Perdikaris, P., Wang, S., and Yang, L. Physics-informed machine learning. *Nature Reviews Physics*, 3(6):422–440, 2021.
- Kass, R. E. and Raftery, A. E. Bayes factors. *Journal of the american statistical association*, 90(430):773–795, 1995.
- Kermack, W. O. and McKendrick, A. G. A contribution to the mathematical theory of epidemics. *Proceedings of the royal society of london. Series A, Containing papers of a mathematical and physical character*, 115(772):700–721, 1927.
- Khattab, O., Santhanam, K., Li, X. L., Hall, D., Liang, P., Potts, C., and Zaharia, M. Demonstrate-search-predict: Composing retrieval and language models for knowledge-intensive NLP. *arXiv preprint arXiv:2212.14024*, 2022.
- Khattab, O., Singhvi, A., Maheshwari, P., Zhang, Z., Santhanam, K., Vardhamanan, S., Haq, S., Sharma, A., Joshi, T. T., Moazam, H., Miller, H., Zaharia, M., and

- Potts, C. DSPy: Compiling declarative language model calls into self-improving pipelines. 2024.
- Lake, B. M., Salakhutdinov, R., and Tenenbaum, J. B. Human-level concept learning through probabilistic program induction. *Science*, 350(6266):1332–1338, 2015.
- Lavin, A., Krakauer, D., Zenil, H., Gottschlich, J., Mattson, T., Brehmer, J., Anandkumar, A., Choudry, S., Rocki, K., Baydin, A. G., Prunkl, C., Paige, B., Isayev, O., Peterson, E., McMahon, P. L., Macke, J., Cranmer, K., Zhang, J., Wainwright, H., Hanuka, A., Veloso, M., Assefa, S., Zheng, S., and Pfeffer, A. Simulation intelligence: Towards a new generation of scientific methods. *arXiv preprint arXiv:2112.03235*, 2022.
- Lewis, P., Perez, E., Piktus, A., Petroni, F., Karpukhin, V., Goyal, N., Küttler, H., Lewis, M., Yih, W.-t., Rocktäschel, T., et al. Retrieval-augmented generation for knowledge-intensive nlp tasks. *Advances in neural information processing systems*, 33:9459–9474, 2020.
- Li, M. Y., Fox, E., and Goodman, N. Automated statistical model discovery with language models. In *Proceedings of the 41st International Conference on Machine Learning*, volume 235, pp. 27791–27807, 2024.
- Liu, F., Xialiang, T., Yuan, M., Lin, X., Luo, F., Wang, Z., Lu, Z., and Zhang, Q. Evolution of heuristics: Towards efficient automatic algorithm design using large language model. In *Forty-first International Conference on Machine Learning*, 2024.
- Lueckmann, J.-M., Gonçalves, P. J., Bassetto, G., Öcal, K., Nonnenmacher, M., and Macke, J. H. Flexible statistical inference for mechanistic models of neural dynamics. In *Advances in Neural Information Processing Systems*, volume 30, 2017.
- Ma, P., Wang, T.-H., Guo, M., Sun, Z., Tenenbaum, J. B., Rus, D., Gan, C., and Matusik, W. LLM and simulation as bilevel optimizers: A new paradigm to advance physical scientific discovery. In *Proceedings of the 41st International Conference on Machine Learning*, volume 235, pp. 33940–33962, 2024.
- Maddah, E. and Hallow, K. M. A quantitative systems pharmacology model of plasma potassium regulation by the kidney and aldosterone. *Journal of Pharmacokinetics and Pharmacodynamics*, 49(4), 2022.
- Morey, R. D., Romeijn, J.-W., and Rouder, J. N. The philosophy of Bayes factors and the quantification of statistical evidence. *Journal of Mathematical Psychology*, 72: 6–18, 2016.
- Moritz, P., Nishihara, R., Wang, S., Tumanov, A., Liaw, R., Liang, E., Elibol, M., Yang, Z., Paul, W., Jordan, M. I., et al. Ray: A distributed framework for emerging AI applications. In *13th USENIX symposium on operating systems design and implementation (OSDI 18)*, pp. 561–577, 2018.
- Müller, S., Hollmann, N., Arango, S. P., Grabocka, J., and Hutter, F. Transformers can do Bayesian inference. In *International Conference on Learning Representations*, 2022.
- Naesseth, C. A., Lindsten, F., Schön, T. B., et al. Elements of sequential monte carlo. *Foundations and Trends® in Machine Learning*, 12(3):307–392, 2019.
- Neal, R. M. Annealed importance sampling. *Statistics and computing*, 11(2):125–139, 2001.
- Novikov, A., Vū, N., Eisenberger, M., Dupont, E., Huang, P.-S., Wagner, A. Z., Shirobokov, S., Kozlovskii, B., Ruiz, F. J. R., Mehrabian, A., Kumar, M. P., See, A., Chaudhuri, S., Holland, G., Davies, A., Nowozin, S., Kohli, P., and Balog, M. AlphaEvolve: A coding agent for scientific and algorithmic discovery, 2025.
- OpenAI. Introducing GPT-5, 2025. <https://openai.com/index/introducing-gpt-5/> [Accessed: 2026-01-23].
- pandas development team, T. pandas-dev/pandas: Pandas, 2020. URL <https://doi.org/10.5281/zenodo.3509134>.
- Papamakarios, G. and Murray, I. Fast  $\epsilon$ -free inference of simulation models with bayesian conditional density estimation. *Advances in neural information processing systems*, 29, 2016.
- Papamakarios, G., Sterratt, D., and Murray, I. Sequential neural likelihood: Fast likelihood-free inference with autoregressive flows. In *The 22nd international conference on artificial intelligence and statistics*, pp. 837–848, 2019.
- Parisotto, E., rahman Mohamed, A., Singh, R., Li, L., Zhou, D., and Kohli, P. Neuro-symbolic program synthesis. In *International Conference on Learning Representations*, 2017.
- Paszke, A., Gross, S., Massa, F., Lerer, A., Bradbury, J., Chanan, G., Killeen, T., Lin, Z., Gimelshein, N., Antiga, L., Desmaison, A., Kopf, A., Yang, E., DeVito, Z., Raison, M., Tejani, A., Chilamkurthy, S., Steiner, B., Fang, L., Bai, J., and Chintala, S. PyTorch: An imperative style, high-performance deep learning library. In *Advances in Neural Information Processing Systems*, volume 32, 2019.

- Pospischil, M., Toledo-Rodriguez, M., Monier, C., Piskowska, Z., Bal, T., Frégnac, Y., Markram, H., and Destexhe, A. Minimal Hodgkin–Huxley type models for different classes of cortical and thalamic neurons. *Biological cybernetics*, 99:427–441, 2008.
- R Core Team. *R: A Language and Environment for Statistical Computing*. R Foundation for Statistical Computing, Vienna, Austria, 2025. URL <https://www.R-project.org/>.
- Rackauckas, C., Ma, Y., Martensen, J., Warner, C., Zubov, K., Supekar, R., Skinner, D., and Ramadhan, A. Universal differential equations for scientific machine learning. *arXiv preprint arXiv:2001.04385*, 2020.
- Raissi, M., Perdikaris, P., and Karniadakis, G. E. Physics-informed neural networks: A deep learning framework for solving forward and inverse problems involving nonlinear partial differential equations. *Journal of Computational physics*, 378:686–707, 2019.
- Rmus, M., Jagadish, A. K., Mathony, M., Ludwig, T., and Schulz, E. Generating computational cognitive models using large language models. In *The Thirty-ninth Annual Conference on Neural Information Processing Systems*, 2025.
- Robert, C. P., Casella, G., and Casella, G. *Monte Carlo statistical methods*, volume 2. Springer, 1999.
- Romera-Paredes, B., Barekatin, M., Novikov, A., Balog, M., Kumar, M. P., Dupont, E., Ruiz, F. J., Ellenberg, J. S., Wang, P., Fawzi, O., et al. Mathematical discoveries from program search with large language models. *Nature*, 625(7995):468–475, 2024.
- Rudy, S. H., Brunton, S. L., Proctor, J. L., and Kutz, J. N. Data-driven discovery of partial differential equations. *Science advances*, 3(4):e1602614, 2017.
- Schmidt, M. and Lipson, H. Distilling free-form natural laws from experimental data. *Science*, 324(5923):81–85, 2009.
- Schröder, C. and Macke, J. H. Simultaneous identification of models and parameters of scientific simulators. In *Proceedings of the 41st International Conference on Machine Learning*, volume 235, pp. 43895–43927, 2024.
- Shojaee, P., Meidani, K., Gupta, S., Farimani, A. B., and Reddy, C. K. LLM-SR: Scientific equation discovery via programming with large language models. In *The Thirteenth International Conference on Learning Representations*, 2025.
- Tilbury, R., Kwon, D., Haydaroglu, A., Ratliff, J., Schmutz, V., Carandini, M., Miller, K., Stachenfeld, K., and Harris, K. D. AI-discovered tuning laws explain neuronal population code geometry. 2025.
- Udrescu, S.-M. and Tegmark, M. AI Feynman: A physics-inspired method for symbolic regression. *Science advances*, 6(16):eaay2631, 2020.
- Vetter, J., Gloeckler, M., Gedon, D., and Macke, J. H. Effortless, simulation-efficient bayesian inference using tabular foundation models. In *The Thirty-ninth Annual Conference on Neural Information Processing Systems*, 2025.
- Wang, W., Hallow, K., and James, D. A tutorial on RxODE: simulating differential equation pharmacometric models in r. *CPT: pharmacometrics & systems pharmacology*, 5(1):3–10, 2016.
- Winsberg, E. *Science in the age of computer simulation*. University of Chicago Press, 2019.
- Zhang, R. Funsearch, 2024. URL <https://github.com/RayZhjh/funsearch>. GitHub repository [Accessed: 2026-01-26].

## A. Software and Computational Resources

All methods are implemented in Python. For general computations, NumPy (Harris et al., 2020) and PyTorch (Paszke et al., 2019) are used. Plotting is performed using Matplotlib (Hunter, 2007). To store and handle experimental results, we employ pandas (pandas development team, 2020). NLE and NPE are performed using SBI’s (Boelts et al., 2025) implementation of the corresponding methods. In the kidney experiment (Sec. 4.3), the models are implemented in R (R Core Team, 2025). To parallelize the evaluation of multiple particles in ModelSMC, we use Ray (Moritz et al., 2018). LLMs are accessed via DSPy (Khattab et al., 2022; 2024), which automatically assembles prompts and returns structured outputs with named fields. Unless stated otherwise, we use GPT-5-mini (OpenAI, 2025) as the underlying language model for both model propagation and feedback generation (Sec. D.3). Code is available at <https://github.com/mackelab/ModelSMC>.

NPE-PFN (Sec. D.1) and NLE-PFN (Sec. D.2) are run on an A100 GPU with 40GB of memory with associated CPUs. NLE and NPE are run on the CPUs only. The particle propagation and evaluation in ModelSMC can be parallelized. In our experiments, we run up to five particles in parallel. In contrast, the baseline method ModelSMC  $N=1$  and FunSearch+ are run sequentially.

## B. Derivation of ModelSMC Weights from a Static Bayesian Target

This section derives the weighting rule used in ModelSMC from a Bayesian posterior over model programs. The derivation makes explicit how likelihood-based weights arise from an SMC construction, with an underlying static inference problem.

**Inference target.** As defined in Sec. 3.2, given observed data  $\mathbf{x}_o = \{(x_o^j, c_o^j)\}_{j=1}^M$ , the target posterior over models is

$$p(m \mid \mathbf{x}_o) \propto p(\mathbf{x}_o \mid m)p(m), \quad (\text{B-1})$$

with marginal likelihood

$$p(\mathbf{x}_o \mid m) = \prod_{j=1}^M p(x_o^j \mid m), \quad p(x_o^j \mid m) = \int p(\theta) p(x_o^j \mid m, \theta, c_o^j) d\theta. \quad (\text{B-2})$$

The prior  $p(m)$  is implicit and corresponds to the marginal distribution over models induced by the LLM-based generative process in the absence of conditioning on observed data.

For notational simplicity, we drop the explicit conditioning on the observed context  $c_o^j$ , including particle-specific feedback variables, for the remainder of the derivation. This corresponds to an idealized setting in which the model proposal distribution depends only on the previously generated model. In practice, the proposal is conditioned on additional contextual information, which leads to approximate rather than exact importance weights (see Remarks below at the end of this section).

**Artificial SMC target distribution.** To apply SMC, we introduce an artificial sequence of latent variables  $(m_1, \dots, m_K)$ , where each  $m_k$  represents a candidate model. We define the unnormalized target distribution on the extended space as

$$\tilde{\pi}(m_{1:K}) := p(m_{1:K}, \mathbf{x}_o) = \prod_{k=1}^K p(m_k \mid m_{1:k-1}) p(\mathbf{x}_o \mid m_k). \quad (\text{B-3})$$

The corresponding normalized target is

$$\pi(m_{1:K}) = \frac{\tilde{\pi}(m_{1:K})}{Z}, \quad Z = p(\mathbf{x}_o)^K. \quad (\text{B-4})$$

Marginalizing  $\pi(m_{1:K})$  over  $m_{1:k-1}$  yields the posterior over models under the LLM-induced prior,  $p_{\text{LLM}}(m_k \mid \mathbf{x}_o)$  for every  $k$ .

Thus, the sequence is purely algorithmic and does not represent a temporal evolution of the system.

**Proposal distribution.** At iteration  $k$ , ModelSMC generates a new model using the same LLM-based generative mechanism. In practice, this proposal is conditioned on the previous model, particle-specific feedback, and task context, yielding

$$q_k(m_k | m_{1:k-1}) := p_{\text{LLM}}(m_k | m_{1:k-1}, c_{1:k-1}, c_{\text{task}}). \quad (\text{B-5})$$

For the purpose of the derivation, we absorb all contextual variables into the conditioning and consider an idealized proposal that depends only on  $m_{1:k-1}$ .

**Incremental importance weights.** The standard SMC incremental weight is

$$\tilde{w}_k = \frac{\tilde{\pi}(m_{1:k})}{\tilde{\pi}(m_{1:k-1}) q_k(m_k | m_{1:k-1})}. \quad (\text{B-6})$$

Using Eq. B-3, we obtain

$$\tilde{w}_k = \frac{\prod_{t=1}^k p(m_t | m_{1:t-1}) p(x_o | m_t)}{\left( \prod_{t=1}^{k-1} p(m_t | m_{1:t-1}) p(x_o | m_t) \right) q_k(m_k | m_{1:k-1})} \quad (\text{B-7})$$

$$= \frac{p(m_k | m_{1:k-1}) p(x_o | m_k)}{q_k(m_k | m_{1:k-1})}. \quad (\text{B-8})$$

We refer to this as a prior-matching proposal when the proposal coincides with the conditional generative distribution defining the implicit model prior in an idealized setting, i.e.,

$$q_k(m_k | m_{1:k-1}) = p(m_k | m_{1:k-1}). \quad (\text{B-9})$$

Under this assumption, the transition terms cancel exactly, yielding the idealized incremental weight

$$\tilde{w}_k = p(x_o | m_k). \quad (\text{B-10})$$

In practice, the proposal is conditioned on additional contextual information (e.g., data-dependent feedback, task context, or finite context windows), and the exact incremental weight would take the form

$$\tilde{w}_k^{\text{true}} = p(x_o | m_k) \frac{p(m_k | m_{1:k-1})}{q_k(m_k | m_{1:k-1}, x_o, c_{1:k-1})}. \quad (\text{B-11})$$

Because this context-conditioned proposal density is implicit and intractable for large language models, ModelSMC omits the correction factor and uses  $p(x_o | m_k)$  as a practical, approximate importance weight.

**Resulting weighting rule.** Thus, under a prior-matching proposal, the incremental SMC weight at iteration  $k$  is precisely the marginal likelihood of the newly proposed model. This yields the weighting rule used in ModelSMC as the likelihood

$$\tilde{w}(m) \propto p(x_o | m). \quad (\text{B-12})$$

**Factorization and numerical stabilization.** Assuming iid observed data  $x_o$ ,

$$p(x_o | m) = \prod_{j=1}^M p(x_o^j | m). \quad (\text{B-13})$$

In practice, ModelSMC uses the normalized geometric mean

$$\tilde{w}(m) = \left( \prod_{j=1}^M p(x_o^j | m) \right)^{1/M}, \quad (\text{B-14})$$

which preserves particle ordering while improving numerical stability for large  $M$ .

**Remarks.**

- **Implicit model prior.** The prior  $p(m)$  is implicit and defined by the marginal distribution over models induced by the LLM generative process. The proposal distribution corresponds to its conditional transitions. ModelSMC therefore performs inference under this implicit prior rather than an explicit analytic one.
- **Approximate prior matching.** The derivation assumes an idealized prior-matching proposal that ignores contextual conditioning. In practice, the LLM proposal depends on feedback and task-specific context, so the exact importance ratio for the SMC weight would additionally include a proposal correction term. Because this proposal density is implicit and intractable, ModelSMC uses likelihood-based weights as a practical approximation, corresponding to inference under an implicit LLM-induced prior.
- **Static target.** The sequence  $(m_1, \dots, m_K)$  is artificial and introduced solely to enable SMC; all marginals correspond to the same static posterior  $p(m | x_o)$ .
- **Tempering extension.** The current formulation uses the full likelihood  $p(x_o | m_k)$  at every iteration. This can be generalized by introducing a schedule  $\beta_1 \leq \dots \leq \beta_K = 1$  and replacing the target at iteration  $k$  with  $p(x_o | m_k)^{\beta_k}$ , recovering a standard tempered SMC sampler (Del Moral et al., 2006). The existing temperature parameter  $\tau$  (Eq. D-39) could be adapted to serve this role.

**C. Proof of ModelSMC Convergence**

**Theorem C.1** (restated Theorem 3.1). *Let  $\pi(m) \propto p(x_o|m)p(m)$  be a fixed target distribution over models, and let  $q(m'|m)$  denote an idealized proposal kernel induced by the propagation step. Assume (i) support coverage, i.e., any  $m$  with  $\pi(m) > 0$  can be generated with non-zero probability; (ii) uniformly bounded importance weights; (iii) conditional independence of propagated particles given resampling; and (iv) exact likelihood evaluation, i.e., the importance weights are computed using the true marginal likelihood  $p(x_o|m)$ . Let  $\{(m^i, w^i)\}_{i=1}^N$  be the particle population at a fixed iteration. Then, for any bounded test function  $\varphi$ ,*

$$\sum_{i=1}^N w^i \varphi(m^i) \xrightarrow{\mathbb{P}} \mathbb{E}_\pi[\varphi(m)] \quad \text{as } N \rightarrow \infty, \quad (\text{C-15})$$

with asymptotic variance  $\mathcal{O}(1/N)$ . The result holds in the presence of resampling.

**Discussion of assumptions.**

- **Assumption (i)** (support coverage) requires that the proposal induced by the LLM assigns non-zero probability to any model with non-zero posterior mass. This assumption cannot be verified formally and depends critically on the expressive capacity and training of the underlying LLM. In practice, we assume that a large class of scientifically meaningful models, including those commonly used in the literature, their combinations, and moderate extrapolations thereof, lie within the effective support of the proposal distribution. The use of textual feedback and task-specific prompts allows the proposal to be steered toward relevant regions of model space, but does not guarantee full coverage. If this assumption is violated, ModelSMC converges to the posterior restricted to the subset of models reachable by the proposal, resulting in asymptotic bias.
- **Assumption (ii)** (uniformly bounded importance weights) ensures finite variance of the Monte Carlo estimator. While difficult to verify formally, it is encouraged in ModelSMC by finite surrogate likelihood outputs, and normalization via a geometric mean across observations.
- **Assumption (iii)** is standard in SMC analyses and is satisfied by resampling followed by conditionally independent propagation (Del Moral, 2004). In ModelSMC, propagation additionally depends on particle context, so strict conditional independence is not fully met in practice. The theorem therefore characterizes an idealized setting that serves as a reference point for the algorithm’s behavior.
- **Assumption (iv)** formalizes an idealized setting in which the marginal likelihood  $p(x_o|m)$  is available exactly. In ModelSMC, this likelihood is approximated using a surrogate density estimator using NLE or NLE-PFN (Papamakarios et al., 2019), see Sec. D.2. The theorem therefore characterizes the asymptotic behavior of an idealized sampler and serves as a reference point for the practical algorithm, as is standard in analyses of likelihood-free SMC methods (Del Moral et al., 2006).

The following argument establishes consistency for an idealized importance sampling or SMC scheme in which the proposal distribution  $q_k$  is known and used to compute exact importance weights. In ModelSMC, the proposal is implicit and context-dependent, so the theorem applies to the corresponding idealized sampler that motivates the practical algorithm.

*Proof.* The proof follows classical importance sampling arguments and their extension to SMC samplers for static target distributions, adapted to the ModelSMC setting (Robert et al., 1999; Del Moral, 2004; Del Moral et al., 2006).

**Step 1: Target expectation and proposal identity.** Fix an iteration  $k$ . Conditional on the resampling step at iteration  $k - 1$ , the propagation step induces a proposal distribution

$$q_k(m) := p_{\text{LLM}}(m \mid m_{k-1}), \quad (\text{C-16})$$

where  $m_{k-1}$  denotes a resampled ancestor. By assumption (i), the support of  $q_k$  contains the support of  $\pi$ .

For any bounded test function  $\varphi$ , we have

$$\mathbb{E}_\pi[\varphi(m)] = \int \varphi(m) \pi(m) dm = \int \varphi(m) \frac{\pi(m)}{q_k(m)} q_k(m) dm = \mathbb{E}_{q_k} \left[ \frac{\pi(m)}{q_k(m)} \varphi(m) \right]. \quad (\text{C-17})$$

**Step 2: Importance sampling estimator.** Let  $m_1, \dots, m_N$  be i.i.d. samples from  $q_k(m)$ . Define (unnormalized) importance weights

$$\tilde{w}_i = \frac{\pi(m_i)}{q_k(m_i)}, \quad w_i = \frac{\tilde{w}_i}{\sum_{j=1}^N \tilde{w}_j}. \quad (\text{C-18})$$

The corresponding estimator is

$$\hat{I}_N := \sum_{i=1}^N w_i \varphi(m_i). \quad (\text{C-19})$$

By the strong law of large numbers,

$$\sum_{i=1}^N w_i \varphi(m_i) \xrightarrow{\text{a.s.}} \mathbb{E}_{q_k} \left[ \frac{\pi(m)}{q_k(m)} \varphi(m) \right] = \mathbb{E}_\pi[\varphi(m)], \quad (\text{C-20})$$

$$\sum_{i=1}^N w_i \xrightarrow{\text{a.s.}} \mathbb{E}_{q_k} \left[ \frac{\pi(m)}{q_k(m)} \right] = \int \pi(m) dm = 1. \quad (\text{C-21})$$

Hence  $\hat{I}_N \rightarrow \mathbb{E}_\pi[\varphi(m)]$  almost surely.

**Step 3: Variance decomposition.** Define the random variables

$$Z_i := \frac{\pi(m_i)}{q_k(m_i)} \varphi(m_i), \quad m_i \sim q_k \text{ i.i.d.} \quad (\text{C-22})$$

Then

$$\frac{1}{N} \sum_{i=1}^N Z_i \xrightarrow{\text{a.s.}} \mathbb{E}_\pi[\varphi(m)]. \quad (\text{C-23})$$

Moreover,

$$\text{Var}(\hat{I}_N) = \frac{1}{N} \text{Var}(Z_1). \quad (\text{C-24})$$

**Step 4: Variance goes to zero.** By Assumption (ii) (uniformly bounded importance weights) and boundedness of  $\varphi$ , there exists  $C < \infty$  such that

$$\left| \frac{\pi(m)}{q_k(m)} \varphi(m) \right| \leq C \quad \text{for all } m. \quad (\text{C-25})$$

Hence  $\text{Var}(Z_1) \leq C^2$ , and therefore

$$\text{Var}(\hat{I}_N) = \text{Var}\left(\frac{1}{N} \sum_{i=1}^N Z_i\right) \leq \frac{C^2}{N} = \mathcal{O}(1/N) \rightarrow 0. \quad (\text{C-26})$$

**Step 5: Convergence in probability (Chebyshev).** For any  $\varepsilon > 0$ , Chebyshev’s inequality yields

$$\mathbb{P}\left(\left|\hat{I}_N - \mathbb{E}_\pi[\varphi(m)]\right| \geq \varepsilon\right) \leq \frac{\text{Var}(\hat{I}_N)}{\varepsilon^2} \leq \frac{C^2}{N\varepsilon^2}, \quad (\text{C-27})$$

which converges to zero as  $N \rightarrow \infty$ . This establishes convergence in probability of the importance sampling estimator to  $\mathbb{E}_\pi[\varphi(m)]$ .

**Step 6: Effect of resampling.** The resampling step replaces the weighted particle system by an equally weighted one whose empirical measure is unbiased. Under Assumption (iii) (conditional independence of propagated particles given resampling) and bounded importance weights, resampling does not change the limit of the estimator and introduces additional variance of order  $\mathcal{O}(1/N)$  only. Therefore, resampling preserves convergence in probability and the Monte Carlo rate.

**Step 7: Importance sampling vs. SMC (path-space argument).** ModelSMC performs SMC updates with incremental weights of the form

$$w_k = \frac{\pi_k(m_k)}{\pi_{k-1}(m_{k-1}) q_k(m_k | m_{k-1})}, \quad (\text{C-28})$$

where  $\{\pi_k\}$  is an artificial sequence of target distributions whose marginal at iteration  $k$  is  $\pi$ . Viewing SMC as importance sampling on the extended path space  $(m_0, \dots, m_k)$ , the product of incremental weights along a trajectory equals the standard importance weight  $\pi(m_k)/q_k(m_k)$  for the marginal distribution. Hence, analyzing the corresponding importance sampling estimator suffices to establish consistency of the SMC estimator.

**Step 8: Conclusion.** Combining the above steps, we obtain that

$$\sum_{i=1}^N w^i \varphi(m^i) \xrightarrow{\mathbb{P}} \mathbb{E}_\pi[\varphi(m)] \quad \text{as } N \rightarrow \infty, \quad (\text{C-29})$$

with asymptotic variance  $\mathcal{O}(1/N)$ . Thus, ModelSMC provides a consistent Monte Carlo approximation of the posterior  $p(m | \mathbf{x}_o)$ .  $\square$

### Remarks.

- **Mixture proposal.** The mixture kernel in Algorithm 1 clones a fraction of particles while propagating the remainder via the LLM. Since cloned particles retain their previous weights and the overall kernel satisfies the support coverage assumption as  $N \rightarrow \infty$ , this does not affect the validity of the convergence argument.
- **Idealized setting.** The theorem characterizes the asymptotic behavior of an idealized ModelSMC sampler with exact importance weights. The implemented algorithm uses approximate weights due to implicit, context-conditioned LLM proposals, and should therefore be interpreted as an approximation to this idealized sampler.
- **Prompt engineering and proposal quality.** Prompt design affects the proposal distribution implicitly by shaping the inductive biases of the LLM. From the perspective of the theorem, prompt engineering serves as a practical mechanism to improve support coverage and reduce weight variance, analogous to hand-crafted proposal kernels in traditional Monte Carlo methods. It influences finite-sample efficiency but does not affect the asymptotic consistency result.

## D. Method Details

### D.1. Parameter Estimation

ModelSMC does not require the value of the external parameters  $\theta$  for the model discovery process. Since many downstream applications require parameter estimation, we estimate the parameter values  $\hat{\theta}$  that best explain the observed data. For an observation  $x_o$  and associated context  $c_o$ , we estimate  $\hat{\theta}_o$  by maximizing the posterior  $p(\theta|x, c, m)$  with respect to  $\theta$  as

$$\hat{\theta}_o = \arg \max_{\theta \in \Theta} \log p(\theta | x_o, c_o, m). \quad (\text{D-30})$$

To simplify notation, we drop the conditioning on the discovered model for the remainder of this section. The key ingredient for estimating  $\hat{\theta}_o$  via Eq. D-30 is access to the posterior  $p(\theta|x, c)$ , which in practice is usually intractable. Therefore, we use a surrogate model

$$p_\psi(\theta | x, c) \approx p(\theta | x, c). \quad (\text{D-31})$$

One approach for obtaining  $p_\psi$  is Neural Posterior Estimation (Lueckmann et al., 2017; Papamakarios & Murray, 2016, NPE) which trains a density estimator  $p_\psi$  from scratch using a training set of  $n_{\text{sim}}$  synthetic samples

$$\mathcal{D} = \{(\theta_j \sim p(\theta), c_j \sim p(c), x_j = m(c_j, \theta_j) \sim p(x | m(\theta, c)))\}_{j=1}^{n_{\text{sim}}}. \quad (\text{D-32})$$

Once  $p_\psi$  is trained, the expression in Eq. D-30 is estimated by drawing  $n_{\text{post}}$  samples from  $p_\psi$  and selecting the sample that maximizes  $p_\psi(\theta|x, c)$

$$\hat{\theta}_o = \arg \max_{\theta \in \Theta_o} \log p_\psi(\theta | x_o, c_o), \quad \text{with } \Theta_o = \{\theta_l \sim p_\psi(\theta | x_o, c_o)\}_{l=1}^{n_{\text{post}}}. \quad (\text{D-33})$$

An alternative to NPE is NPE-PFN (Vetter et al., 2025). NPE-PFN employs TabPFN as a conditional density estimator. TabPFN (Hollmann et al., 2025) is a Prior-data Fitted Network (Müller et al., 2022) for tabular data, which provides one-dimensional density estimates and can be autoregressively extended for higher-dimensional densities. The key difference between NPE and NPE-PFN is that NPE-PFN does not train a new surrogate model but uses  $\mathcal{D}$  (see, Eq. D-32) as an in-context dataset for the pretrained TabPFN model. Hence, NPE-PFN allows for training-free posterior estimation.

Following Vetter et al. (2025) and adapting to the case of additional external context  $c_o$ , the posterior can be decomposed into a product over the parameter dimensions as

$$p(\theta|x_o, c_o) \approx \prod_{j=1}^{d_\theta} q_\psi(\theta_j | \theta_{<j}, x_o, c_o, \mathcal{D}_{<j}). \quad (\text{D-34})$$

For a  $d_\theta$ -dimensional parameter space,  $\theta_j$  is the  $j$ -th component of  $\theta$ , and  $\theta_{<j}$  the components of  $\theta$  up to, but not including, the  $j$ -th. Analogously,  $\mathcal{D}_{<j}$  is defined as  $\mathcal{D}_{<j} = \{\theta_j^i, [\theta_{<j}^i, x^i, c^i] : (\theta^i, x^i, c^i) \in \mathcal{D}\}$ . In the setting of NPE-PFN  $q_\psi$  is a one-dimensional density estimate by TabPFN. To sample from the approximated posterior Eq. D-34, the individual dimensions of  $\theta$  are sampled recursively.

The parameter estimation scheme Eq. D-30 used for NPE can also be applied with NPE-PFN. For high-dimensional parameter spaces, however, the recursive sampling and density estimation (Eq. D-34) for  $n_{\text{post}}$  posterior samples can slow down the discovery process. To reduce the computational costs of the parameter estimation, we exploit NPE-PFNs factorization of the posterior Eq. D-34 and introduce a new strategy for estimating  $\hat{\theta}_o$  which is based on temperature-scaling the posterior.

Temperature-scaling refers to exponentiating a density with an exponent of  $\frac{1}{T}$ , with the temperature  $T > 0$ . Applying this transformation to a density leaves the positions of the modes, i.e., the local maxima, unchanged. Furthermore, for  $T \ll 1$  the temperature-scaled density becomes localized around the mode with the highest density value in the original density. Sampling from the temperature-scaled distribution accordingly produces samples that have a high density under the original distribution.

Sampling from the temperature-scaled posterior at  $T \ll 1$  instead of the posterior itself can significantly reduce the necessary amount of posterior samples  $n_{\text{post}}$  in Eq. D-33 as all samples are close to the posterior mode with the highest density value. Therefore, we temperature-scale the posterior to obtain

$$p(\theta|x_o, c_o)^{\frac{1}{T}} \approx \prod_{j=1}^{d_\theta} q_\psi(\theta_j | \theta_{<j}, x_o, c_o, \mathcal{D}_{<j})^{\frac{1}{T}}. \quad (\text{D-35})$$

Crucially, Eq. D-35 only requires to power-scale the one-dimensional factors in the product rather than the full, potentially high-dimensional, posterior itself. In our experiments, we draw one sample from the temperature-scaled posterior and use it as  $\hat{\theta}_o$ . Drawing only one sample from the temperature-scaled posterior reduces the computational cost of the parameter estimation from  $n_{\text{post}}$  sampling and density estimation steps to a single sampling step. Therefore, this parameter estimation approach exploits the factorization of the posterior in NPE-PFN and significantly reduces the computational costs of the parameter estimation.

## D.2. Estimation of Resampling Weights: Likelihood Estimation

Eq. 4 defines the resampling weight of a particle as the likelihood of the observed data  $x_0$  under the model  $m$ , marginalized over the external parameters  $\theta$ . In practice, the likelihood  $p(x|\theta, c, m)$  is intractable. Therefore, we use a surrogate model  $p_\phi(x|\theta, c, m) \approx p(x|\theta, c, m)$  in the computation of Eq. 4. For simplicity, we drop the conditioning on  $m$  for the remainder of this section.

One approach to learn a surrogate model is to apply Neural Likelihood Estimation (Papamakarios et al., 2019, NLE). NLE uses the training set  $\mathcal{D}$  (see Eq. D-32) to train the surrogate model  $p_\phi(x|\theta, c, m)$  via maximum likelihood training. An alternative to NLE is to adapt NPE-PFN (Vetter et al., 2025) to likelihood estimation. We denote this approach as NLE-PFN. Compared to Eq. D-34, NLE-PFN effectively interchanges  $\theta$  and  $x$ , yielding

$$p(x|\theta, c) \approx \prod_{j=1}^{d_x} q_\psi(x_j | x_{<j}, \theta, c, \mathcal{B}_{<j}), \quad (\text{D-36})$$

where  $d_x$  denotes the dimensionality of the observation space,  $x_j$  the  $j$ -th component of the observation, and  $x_{<j}$  the components of  $x$  up to, but not including, the  $j$ -th. The in-context dataset  $\mathcal{B}$  is defined as  $\mathcal{B}_{<j} = \{x_j^i, [x_{<j}^i, \theta^i, c^i] : (\theta^i, x^i, c^i) \in \mathcal{D}\}$ . As in NPE-PFN, each factor in Eq. D-36 is estimated by a one-dimensional density estimate from TabPFN (Hollmann et al., 2025).

With the likelihood surrogate model  $p_\phi(x | \theta, c, m)$ , Eq. 4 can be estimated by the Monte Carlo estimate

$$p(x_o^i | m_k^i) \approx \frac{1}{B} \sum_{b=1}^B p(x_o^i | m_k^i, \theta_b, c_0^i), \quad \theta_b \stackrel{i.i.d.}{\sim} p(\theta), \quad \forall b = 1, \dots, B. \quad (\text{D-37})$$

For high-dimensional observations, we can use summary statistics  $s : X \rightarrow \mathbb{R}^d$  with  $d \ll d_x$  (Lueckmann et al., 2017). Assuming that  $s(x)$  retains most of the relevant information about  $x$ , the approximation of the likelihood changes to

$$p(x|\theta, c) \approx p_\phi(s(x)|\theta, c). \quad (\text{D-38})$$

Evaluating Eq. D-37 for each observed instance  $(x_o^j, c_o^j) \in \mathbf{x}_o$  allows us to compute the unnormalized resampling weight  $\tilde{w}_k^i$  (Eq. 5) of a model  $m_k^i$ . In practice, we use the slightly adapted definition Eq. D-39 of  $\tilde{w}_k^i$  of the form

$$\tilde{w}_k^i \propto \exp \left( \frac{1}{\tau} \log \left( \left( \prod_{j=1}^M p(x_o^j | m_k^i) \right)^{1/M} \right) \right). \quad (\text{D-39})$$

The temperature parameter  $\tau$  in Eq. D-39 controls the bias of the resampling step. For  $\tau \ll 1$ , particles explaining the data well are favored, whereas for  $\tau \gg 1$ , the selection becomes more uniform across all particles. Unless stated otherwise, the temperature is set to  $\tau = 1$  in all experiments. Importantly, the temperatures  $T$  and  $\tau$  used in Eq. D-39 and Eq. D-35 are two distinct hyperparameters.

In the definition of the resampling weights used by ModelSMC (Eq. 5 and Eq. D-39) the geometric mean over all observed instances is used rather than the direct product. First, the geometric mean yields weights whose magnitudes are invariant to the number of observed samples. Second, in practice, this approach reduces the risk of numerical instabilities.

## D.3. Prompting Strategy

In the propagation step of ModelSMC (see Algorithm 1 and Sec. 3.3), an LLM is used as a conditional sampler for implementations of models, implicitly synthesizing new models. To obtain meaningful implementations, we condition the LLM on text-based conditions incorporating information about previously generated models and the task to solve.

Passing information about models generated earlier in the discovery process, especially their implementations, to the LLM, is a well-established strategy in LLM-based model discovery (Holt et al., 2025; Castro et al., 2025; Romera-Paredes et al., 2024; Agarwal et al., 2025). We follow this general scheme by providing the ancestry of implementations  $m_{k-1}^{a_k^i}$  and the ancestry of performance feedback  $c_{k-1}^{a_k^i}$  to the LLM. Both rely on the ancestry of the resampled particle. Injecting ancestral information in the propagation step enables the LLM to reason about the effect of changes to the models on their performance.

Furthermore, we pass a task-specific context  $c_{\text{task}}$  to the LLM, which does not change over the course of the discovery run. The task-specific context  $c_{\text{task}}$  contains all information about the task. By passing  $c_{\text{task}}$  to the LLM, we aim at triggering the LLM’s broad knowledge base to further improve its ability to provide implementations that solve the given task. ModelSMC structures  $c_{\text{task}}$  into three parts:

1. **System description.** We include all prior information about the task to solve. This includes information about the initial solution provided to ModelSMC or the metrics used to evaluate the generated models. The description also contains information about the scientific domain and about the data used to test the synthesized models.
2. **Signature description.** We collect all information about the framework in which the generated models are evaluated. This includes details such as the interpretation and structure of the model’s input arguments and outputs.
3. **Task description.** This part summarizes the aim of the discovery run and describes how the tasks should be approached (i.e., to reason from previous attempts, use coding standards, or specific coding instructions).

The different parts of  $c_{\text{task}}$  can vary across different applications, depending on the amount of prior knowledge, the environment used to evaluate the code, the scientific domain, and the specifics of the task. For the full prompts, we refer to the supplementary materials.

The generation of contextual feedback  $c_k^i$  of a model  $m_k^i$  (see Algorithm 1) is performed after model simulation, and the numerical performance metrics are computed. The contextual feedback has two stages. In the first stage, the system description and the numerical evaluation metrics are provided to the LLM, which is instructed to diagnose the model performance based on the metrics. This stage also records and provides feedback on any exceptions and errors arising during evaluation. In the second stage, a separate LLM call produces structured feedback conditioned on the diagnosis, the model implementation, the system description, and the evaluation outcomes. The resulting feedback is designed to guide subsequent LLM propagation steps by highlighting concrete directions for model revision.

During model simulation and evaluation, exceptions may arise due to invalid code, numerical instability, non-terminating simulations, or timeouts. Such exceptions are explicitly caught and recorded. When an exception occurs, a structured description of the failure mode (e.g., error messages, timeout events, or invalid outputs) is included in the first-stage diagnosis and propagated to the LLM as part of the contextual feedback. This allows models that failed to receive targeted corrective feedback to be revised if they are later resampled as ancestors, rather than being irreversibly discarded.

## E. Baseline Methods

### E.1. FunSearch+

FunSearch (Romera-Paredes et al., 2024) is an LLM-based evolutionary method to evolve function implementations to improve their performance with respect to an evaluation function. The program database used by FunSearch to store previously generated functions consists of several pools of functions, referred to as islands. Periodically, the worst-performing islands are discarded and reinitialized with a function from the remaining well-performing islands. When generating the prompt to synthesize a new function, FunSearch randomly selects an island and samples  $k$  functions from this island with sampling probabilities based on their score and length. The selected functions are sorted by their scores and inserted into the program skeleton to provide ranked examples to the LLM. Based on this prompt, the LLM is tasked to implement a new function with the goal of generating a higher-scoring function. Newly generated functions are added to the same island from which the functions in the prompt were selected. Therefore, the islands evolve independently between reinitialization steps. A key difference between ModelSMC and FunSearch is that FunSearch selects the functions in the prompt based on the score but does not consider ancestral relations.

As originally proposed for problems from extremal combinatorics, FunSearch does not allow the use of external model parameters  $\theta$ . We therefore include the ability to use and estimate model parameters in FunSearch and denote this extended

version as FunSearch+. Including external model parameters into FunSearch is conceptually inspired by Castro et al. (2025). Castro et al. (2025) applies gradient descent-based optimization on a likelihood-based criterion to estimate the values of the model parameters. The score of a discovered model is given by the validation performance of this criterion, given the optimized parameters. Instead of using gradient-based parameter optimization, we use the parameter estimation approach based on NPE and NPE-PFN described in Sec. D.1. The advantage of using NPE and NPE-PFN to estimate  $\hat{\theta}$  over gradient-based approaches is to obtain posterior estimates for the parameters without requiring differentiable model. Inspired by the use of a likelihood-based score in Castro et al. (2025), we also use a likelihood-based score in FunSearch+, which we define as

$$s = \log \left( \left( \prod_{j=1}^M p_{\phi}(x_o^j | m, c_o^j, \hat{\theta}^j) \right)^{1/M} \right). \quad (\text{E-40})$$

In Eq. E-40,  $\hat{\theta}^j$  denotes the parameter estimate for the observed instance  $(x_o^j, c_o^j) \in \mathbf{x}_o$  and  $p_{\phi}(x|m, c, \theta)$  is a surrogate likelihood for the unknown true likelihood  $p(x|m, c, \theta)$ . The surrogate likelihood is estimated as described in Sec. D.2.

We base our implementation of FunSearch+ on the openly available FunSearch implementation provided by Zhang (2024). Our main modifications include evolving class methods rather than standalone functions and including our parameter estimation (Sec. D.1) and scoring schemes (see Eq. E-40). Zhang (2024) relies on string-based modifications of functions and is therefore tightly coupled to Python code. As a result, unlike ModelSMC, it cannot be readily extended to other programming languages.

## E.2. ModelSMC $N=1$

This baseline method represents alternative LLM-based approaches for model discovery that evolve an initial model in a single trajectory of models. A representative of this class of algorithms is, for example, G-Sim (Holt et al., 2025). ModelSMC  $N=1$  uses the same implementation as ModelSMC (including the definition of the resampling weights), but only samples one particle per iteration and only keeps one particle as a candidate for resampling.

## F. Experimental Details

Here, we provide details on the exact configurations used in the experiments. For a complete list of all settings and details on the implementation, we refer to the accompanying code.

### F.1. Validation of ModelSMC for Model Discovery

The experiment presented in Sec. 4.1 tests the probabilistic inference mechanism underlying ModelSMC without using LLMs to synthesize new models. To implement this, we restrict ModelSMC to select models from a finite model space consisting of 20 predefined candidate models that produce ten-dimensional observations.

#### F.1.1. CANDIDATE MODELS

The candidate models used in this experiment are Gaussian Mixture Models (GMMs). Given the number of mixture components  $n_{\text{comp}} \in \mathbb{N}$ , a set of covariance matrices  $\{\Sigma^i \in \mathbb{R}^{10 \times 10}\}_{i=1}^{n_{\text{comp}}}$ , mean vectors  $\{\mu^i \in \mathbb{R}^{10}\}_{i=1}^{n_{\text{comp}}}$ , and weights  $\{w^i \in \mathbb{R}_+\}_{i=1}^{n_{\text{comp}}}$  with  $\sum_i w^i = 1$ , we define a GMM as

$$p_{\text{GMM}}(x | s, u) = \sum_{i=1}^{n_{\text{comp}}} w^i \cdot \frac{1}{(2\pi)^{d_x/2} \det(s^2 \Sigma^i)^{1/2}} \exp \left( -\frac{1}{2s^2} (x - (s\mu^i + u))^T (\Sigma^i)^{-1} (x - (s\mu^i + u)) \right). \quad (\text{F-41})$$

Here,  $d_x = 10$  is the dimensionality of the data space, and  $s$  and  $u$  are the external parameters of the model: the scale parameter  $s$  is scalar and follows a uniform prior over the interval  $[0.1, 2]$ . The shift parameter  $u$  is a ten-dimensional vector, where all but four components are set to zero. Each of the four non-zero components follows a uniform prior over the interval  $[-2, 2]$ . The non-zero components are sampled uniformly at random when initializing the candidate model and remain unaltered over the discovery run. The external parameters allow to scale and to shift the GMM along selected components to fit it to the observed data. For each candidate model, the configuration of the underlying GMM is randomly

initialized as

$$n_{\text{comp}} \sim \text{Unif}(\{1, 2, \dots, 10\}), \quad (\text{F-42})$$

$$\tilde{w}^i \sim \text{Unif}([0, 1]), \quad w^i = \frac{\tilde{w}^i}{\sum_{j=1}^{n_{\text{comp}}} \tilde{w}^j}, \quad \forall i = 1, \dots, n_{\text{comp}}, \quad (\text{F-43})$$

$$\mu_j^i \sim \text{Unif}([-5, 5]), \quad \forall j = 1, \dots, 10, \quad \forall i = 1, \dots, n_{\text{comp}}, \quad (\text{F-44})$$

$$\tilde{\Sigma}_{jk}^i \sim \text{Unif}([-2, 2]), \quad \forall j, k = 1, \dots, 10, \quad \forall i = 1, \dots, n_{\text{comp}}, \quad (\text{F-45})$$

$$\Sigma^i = \alpha^i \cdot \tilde{\Sigma}^i \left( \tilde{\Sigma}^i \right)^T, \quad \alpha^i \sim \text{Unif}([1, 2]), \quad \forall i = 1, \dots, n_{\text{comp}}. \quad (\text{F-46})$$

In each discovery run, one of the 20 candidate models is selected as the ground truth model  $m^*$ , and observed data is drawn from  $m^*$  with  $s = 1$  and  $u = [0, \dots, 0]$ , i.e., no scaling and shifting is applied.

### F.1.2. EXPERIMENTAL CONFIGURATION

Ten different ground truth models are selected from the set of 20 candidate models. For each ground truth model, ten discovery runs are conducted, each with a different random seed, resulting in a total of 100 discovery runs. The set of candidate models is the same for all discovery runs.

ModelSMC’s resampling weights are estimated using NLE (Papamakarios et al., 2019) with a training set  $\mathcal{D}$  of size 5,000 (Sec. D.2). No additional context is used, i.e., a training instance consists of parameters  $\theta = (s, u)$  drawn from the prior and a simulation  $m(\theta)$ . The observed set  $\mathbf{x}_0$  is of size 1,000 and is drawn from the ground-truth model. To compute the Monte Carlo estimate Eq. D-37,  $B = 2,000$  prior samples are used. We employ sbi’s (Boelts et al., 2025) default hyperparameters for NLE but limit the maximum number of training epochs to 500.

All discovery runs proceed for 30 iterations and cloning probability  $\alpha=1$  (i.e., no new models are proposed by an LLM). In this LLM-free setting, ModelSMC reduces to resampling from the fixed candidate pool according to likelihood-based weights. The particle pool is limited to a maximum size of  $N=50$  particles. Therefore, no new models are generated. To ensure that all candidate models are available for selection by ModelSMC, the resampling weights are computed for all 20 candidate models in the first iteration. In addition to not using an LLM in the propagation step, no text-based performance feedback (Sec. D.3) is generated.

## F.2. SIR Model

We apply ModelSMC to a synthetic dataset where the ground truth simulator model is known. In particular, we use a simple epidemiological SIR model (Kermack & McKendrick, 1927). The SIR model considers three populations—Susceptible, Infected, Recovered—with interactions controlled by two external parameters, a base transmission rate  $\beta$  and a recovery probability  $\gamma$ . In this experiment, we use a time-discretized adaptation of the classical SIR model from Holt et al. (2025).

### F.2.1. DATASET

We use the implementation of the ground truth model by Holt et al. (2025) to generate observed data. Synthetic data is generated by drawing the initial numbers of susceptible, infected, and recovered individuals from the prior distributions specified as (Holt et al., 2025)

$$S_0 \sim \text{Unif}(\{50, 51, \dots, 99, 100\}), \quad I_0 \sim \text{Unif}(\{1, 2, \dots, 4, 5\}), \quad R_0 = 0. \quad (\text{F-47})$$

These initial population sizes define the context  $c = (S_0, I_0, R_0)$ . Given the external parameters  $\beta$  and  $\gamma$ , the population sizes at time step  $t \in \{1, \dots, T\}$  are computed recursively from those at time  $t - 1$ . Let  $N = S_{t-1} + I_{t-1} + R_{t-1}$  and  $p_{\text{inf}} = 1.0 - \exp(-\beta \cdot I_{t-1}/N)$ . New infections and recoveries are drawn as

$$N_{\text{inf}} \sim \text{Binomial}(S_{t-1}, p_{\text{inf}}), \quad N_{\text{rec}} \sim \text{Binomial}(I_{t-1}, \gamma), \quad (\text{F-48})$$

and the state is updated via

$$S_t = S_{t-1} - N_{\text{inf}}, \quad I_t = I_{t-1} + N_{\text{inf}} - N_{\text{rec}}, \quad R_t = R_{t-1} + N_{\text{rec}}. \quad (\text{F-49})$$

Because infections and recoveries are sampled from Binomial distributions, the transitions across time steps are stochastic. In total, the simulation runs for  $T = 60$  time steps, yielding three time series of 61 time steps. The prior distributions for the external parameters follow Holt et al. (2025) and are given by

$$\gamma \sim \text{Unif}([0, 1]), \quad \beta \sim \text{Unif}([0, 2]). \quad (\text{F-50})$$

In our experiments, these priors are fixed for all generated models and are not treated as part of the model. In contrast to Holt et al. (2025), we do not use an LLM to synthesize the dimensionality of the parameter space and the bounds of the uniform priors.

In analogy to the NPE-based parameter estimation scheme applied in (Holt et al., 2025), a single training trajectory drawn from the ground truth model is used to estimate  $\beta$  and  $\gamma$ . For computations of evaluation metrics, including the resampling weights, we use  $x_0$  containing 100 samples drawn from the same generative process.

### F.2.2. EXPERIMENTAL CONFIGURATION

Parameter estimation for  $\beta$  and  $\gamma$  is performed using NPE with a training set of 1,000 synthetic instances (Sec. D.1). Each synthetic training sample consists of a context  $c = (S_0, I_0, R_0)$  drawn from the initial condition priors, parameters  $\theta = (\gamma, \beta)$  drawn from their uniform priors, and an observation  $x = m(\theta, c)$ . The observation is a 183-dimensional vector formed by concatenating the simulated time series of susceptible, infected, and recovered populations.

After training, parameter values are inferred using  $10^4$  samples drawn from the approximate posterior  $p_\psi(\theta|x_o, c_o, m)$  using maximum log-posterior (MAP) criterion (Eq. D-33). Here,  $x_o$  denotes the single observed trajectory generated from the ground-truth data-generating model and  $c_o$  the corresponding initial condition. The resulting parameter estimate for  $\beta$  and  $\gamma$  is fixed and reused for all downstream computations. No summary statistics are applied to the observations.

This estimation procedure is inspired by (Holt et al., 2025) but differs in multiple aspects: In our implementation, the initial condition is explicitly treated as a condition in NPE. Moreover, we normalize the observations and the initial conditions elementwise by the total population size before passing them to the density estimator. Finally, we use a MAP estimate based on posterior samples, whereas Holt et al. (2025) averages posterior samples, which can lead to poor parameter estimates for multimodal posteriors.

Resampling weights for ModelSMC are computed using NLE (Sec. D.2). The training set for NLE is identical to the normalized training set used for NPE in the parameter estimation step. We approximate the marginal likelihood (Eq. D-37) using 2,000 prior samples. ModelSMC runs for up to 20 iterations, with cloning probability  $\alpha=0.7$  (i.e., 15 newly proposed models per iteration). The particle pool is limited to a maximum size of  $N=50$  particles. Discovery runs are terminated if the optimized metric does not improve for more than ten iterations.

The prompts in  $c_{\text{task}}$  (Sec. D.3) are constructed by adapting the prompts used in Holt et al. (2025) to match the specifics of ModelSMC. We follow the same procedure for the program skeleton. Components predicting prior bounds are removed, and the initial simulator model is restricted to return constant population sizes.

For ModelSMC  $N=1$  (see Sec. E.2), up to 150 models are generated with early stopping if no improvement is detected for more than 100 iterations. FunSearch+ (Sec. E.1) generates 150 functions and also uses the same evaluation pipeline as the other two approaches. All methods include up to five previously generated implementations, i.e., ancestors, to the LLM. To compute the results in Table 1, all methods are run with ten different initial random seeds. The two baseline methods use the same parameter estimation scheme as ModelSMC. For implementation details, we refer to the accompanying code.

## F.3. Pharmacological Kidney Model

### F.3.1. DATASET

The dataset is originally from Dluhy et al. (1972); we use the version provided with the manuscript from Maddah & Hallow (2022). The data contains measured plasma potassium and aldosterone responses to a standardized potassium chloride infusion in healthy humans under controlled dietary conditions. Subjects were assigned to four diet groups defined by low/high potassium (40 vs. 200 mEq/day) and low/high sodium (10 vs. 200 mEq/day) intake for 6–10 days, then received potassium chloride at 0.62 mEq/min for 120 min followed by 180 min recovery. Plasma potassium and aldosterone were sampled at baseline, during infusion (0, 30, 90, 120 min), and after recovery (300 min). This constitutes a total of 40 unique data points. There are no summary statistics used.

As context  $c$  is passed to the model, we give the initial condition of the model. The initial condition is derived from steady-state conditions with normal sodium and potassium intake. The model parameters  $\theta$  are drawn from uniform priors. For details about the bounds of the prior, we refer to the accompanying code.

### F.3.2. EXPERIMENTAL CONFIGURATION

ModelSMC is run for 20 iterations with cloning probability  $\alpha=0.8$  (i.e., 10 newly proposed models per iteration). The particle pool is limited to a maximum size of  $N=50$  particles. If the best resampling weight does not improve for 15 consecutive iterations, the run is terminated early. Parameter estimation is performed using NPE-PFN with temperature-scaled posteriors (Sec. D.1), using temperature  $T = 10^{-5}$  and 2,000 simulator calls per evaluation. Resampling weights are estimated using NLE-PFN (Sec. D.2), and the marginal likelihood estimate in Eq. D-37 is approximated with  $B = 2,000$  prior samples. In each propagation step, up to five previously discovered models are provided as few-shot context to the LLM (Sec. D.3).

For ModelSMC  $N=1$ , the same parameter and weight estimation settings are used, but only a single particle is propagated and retained per iteration. ModelSMC  $N=1$  is run for 100 iterations without early stopping based on lack of improvement. All experiments are performed using fixed, manually defined summary statistics and are evaluated using the negative average log marginal likelihood estimated by NLE-PFN.

## F.4. Hodgkin-Huxley Model

### F.4.1. DATASET

We consider data from the Allen cell types database (Allen Institute for Brain Science, 2015), which consists of 10 in-vitro recordings from a mouse cortex. This data was previously used for parameter inference (Gonçalves et al., 2020; Vetter et al., 2025). We use the same set of seven summary statistics as previously proposed in Gonçalves et al. (2020): Spike count, mean, and standard deviation of the resting potential, and the first four voltage moments, i.e., mean, standard deviation, skew and kurtosis.

The additional context  $c$  passed to the model is a two-dimensional vector containing the initial membrane voltage  $V_0$  and the input current  $I$  to the cell. The prior over the conditions is defined by uniformly drawing the context values from the observed set  $x_0$ . The two context dimensions are drawn independently, resulting in 100 possible combinations of initial voltage and input current. Model parameters  $\theta$  are ten-dimensional vectors with components independently drawn from uniform priors, in the same way as provided in Gonçalves et al. (2020). For details about the bounds of the prior, we refer to the accompanying code.

### F.4.2. EXPERIMENTAL CONFIGURATION

ModelSMC runs for 20 iterations with cloning probability  $\alpha=0.7$  (i.e., 15 newly proposed models per iteration). The particle pool is limited to a maximum size of  $N=50$  particles. If the best resampling weight does not improve for more than 15 iterations, the discovery runs are terminated prematurely. For parameter estimation, we employ NPE-PFN-based parameter estimation utilizing temperature-scaling of the posterior (Sec. D.1). The temperature used for temperature-scaling (Eq. D-35) is  $T = 10^{-5}$ . NPE-PFN uses an in-context dataset  $\mathcal{D}$  (Eq. D-32) of size 5,000. Resampling weights, i.e. likelihood estimates, are obtained using NLE-PFN (Sec. D.2), and Eq. D-37 is estimated with  $B = 2,000$  prior samples. NLE-PFN and NPE-PFN are applied to seven standard summary statistics (Gonçalves et al., 2020) rather than to the full voltage traces. In each propagation step, up to five ancestral samples are prompted to the LLM (Sec. D.3).

For ModelSMC  $N=1$  (Sec. E.2), we use the same configuration for parameter and weight estimation as in ModelSMC, with the difference of only propagating a single particle in each iteration and only considering one particle as a candidate for resampling. ModelSMC  $N=1$  runs for 150 iterations. FunSearch+ (Sec. E.1) generates 150 models and uses up to five previously synthesized models to construct the prompts used for propagation. Per prompt, four new models are generated. The program database consists of ten islands, and reinitialization of the worst-performing islands is performed every four hours. To estimate the parameters of the generated models and to compute the score (Eq. E-40), NPE-PFN and NLE-PFN are used with the same settings as in ModelSMC and ModelSMC  $N=1$ . All three methods are run with ten different initial random seeds to obtain the results presented in Table 1.

## G. Additional Experiments

### G.1. Extended Version of Table 1

Table G-1. **Extended version of Table 1.** Metrics are collected for the best-performing particle from each of the ten discovery runs. Best-performing particles are selected according to the metric which was applied to weight particles during the discovery process. We report the median metric together with a 90% confidence interval. The confidence interval is estimated using a percentile bootstrap:  $10^4$  bootstrap samples of size ten are drawn with replacement from the metric values of the selected particles. The median is computed for each sample, and the 5% and 95% quantiles of the resulting distribution are reported.

	ModelSMC	$-\frac{1}{M} \log p(x_o m)(\downarrow)$ FunSearch+	ModelSMC $N=1$
SIR	<b>-503.37 (-583.33 - -448.45)</b>	-500.00 (-521.88 - -474.78)	-464.17 (-503.99 - -415.40)
Kidney	<b>43.58 (42.53 - 45.10)</b>	N/A	46.29 (45.70 - 47.09)
HH	<b>25.18 (24.91 - 25.59)</b>	28.96 (28.21 - 29.67)	25.95 (25.36 - 26.12)
		$-\frac{1}{M} \log p(x_o \hat{\theta}, m)(\downarrow)$	
SIR	<b>-492.67 (-577.77 - -441.17)</b>	-492.05 (-515.91 - -472.39)	-455.13 (-491.27 - -412.55)
Kidney	<b>55.05 (51.51 - 57.23)</b>	N/A	58.63 (56.48 - 83.43)
HH	15.47 (14.23 - 16.45)	<b>12.05 (10.92 - 12.86)</b>	15.64 (13.59 - 17.73)

### G.2. LLM Token Usage

A metric to assess the effectiveness of an LLM-based model discovery algorithm is how many tokens are passed to and generated by an LLM to synthesize a model with a certain performance on the observed data. To minimize computational costs, the number of tokens needed for a certain performance should be as small as possible. In this section, we examine how ModelSMC performs under this metric compared to the baseline methods (Sec. E.1 and Sec. E.2).

The results in Fig. G-1 are based on the discovery runs evaluated in Sec. 4.2. For each evaluated task and method, the five best-performing runs are selected. For FunSearch+, this selection is based on the score Eq. E-40 and for ModelSMC and ModelSMC  $N=1$  based on the resampling weight Eq. 5. For each run, the globally best performance and total number of used tokens at each iteration are collected. These properties are averaged over the five runs.

Fig. G-1 shows that while the two baselines, ModelSMC  $N=1$  and FunSearch+, both generate 150 functions, the amount of required tokens strongly differs. This discrepancy is expected. In addition to the ancestry of the resampled model, ModelSMC and ModelSMC  $N=1$  pass prompts  $c_{\text{task}}$  and text-based performance evaluations (Sec. D.3) to the LLM in the propagation step. FunSearch+, on the other hand, only provides the code skeleton with the functions sampled from the program database to the LLM. Therefore, FunSearch+ requires fewer input tokens. Furthermore, ModelSMC and ModelSMC  $N=1$  require more output tokens since both generate text-based performance feedback, which is not part of FunSearch+.

At the maximum token budget used by the baselines, ModelSMC performs comparably to the two baseline approaches and, in the case of ModelSMC  $N=1$ , even exceeds its performance in some settings (left panel, bottom row, and right panel, second row of Fig. G-1). Thus, formulating the model discovery process as probabilistic inference does not negatively affect the efficiency of the discovery process compared to the baselines.

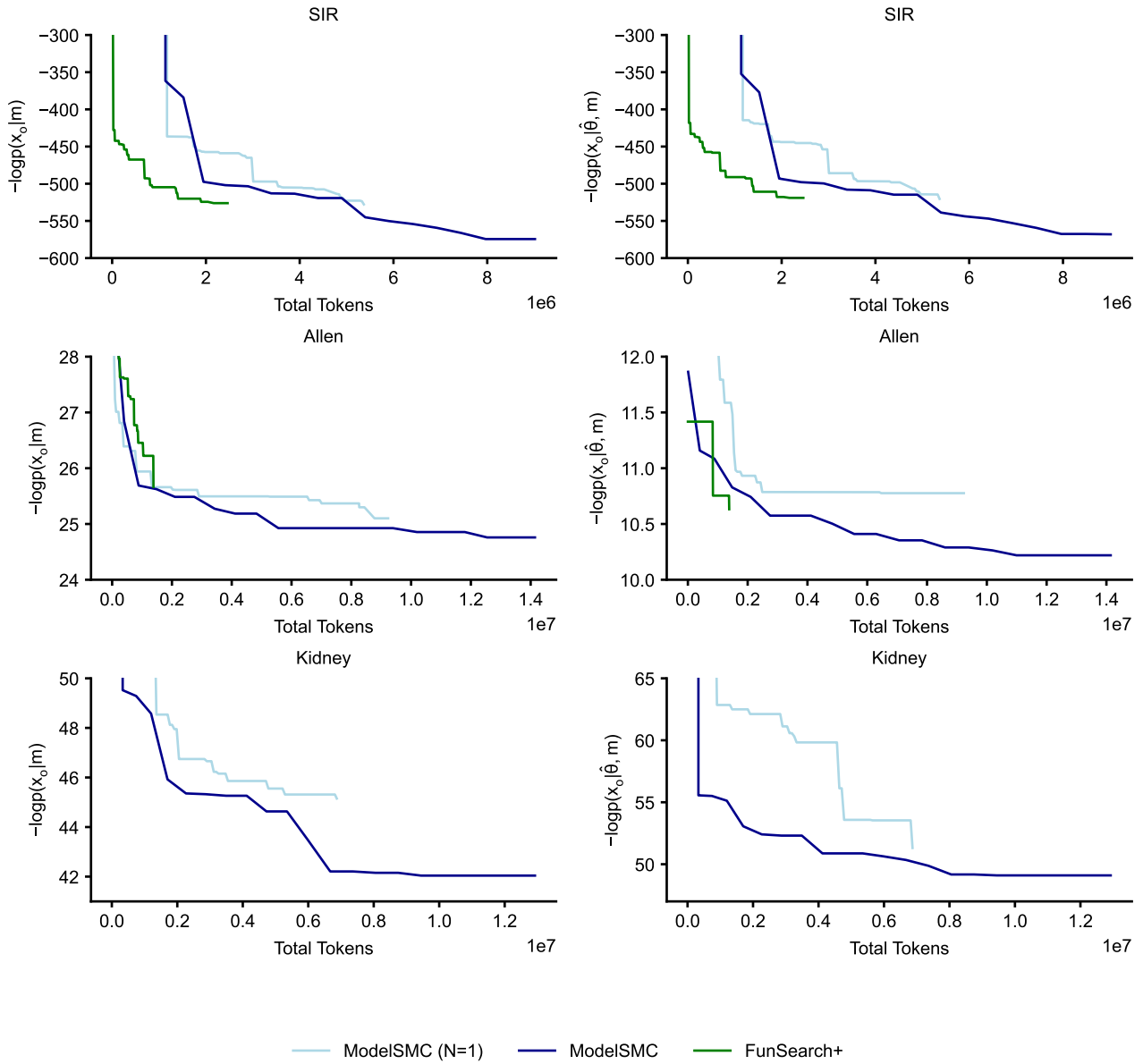


Figure G-1. **Performance of the discovered models as a function of token usage.** Each row corresponds to a task, and each column to a performance metric. Dark blue: ModelSMC. Light Blue: Model SMC  $N=1$ . Green: FunSearch+. The depicted performance metrics and token counts are averaged over the five best discovery runs out of the ten discovery runs conducted for the experiments discussed in Sec. 4.2. First row: Synthetic data from a SIR epidemiological model (Sec. F.2). Second row: Hodgkin-Huxley Model (Sec. 4.4 and Sec. F.4). Third row: Pharmacological kidney model (Sec. 4.3 and Sec. F.3). Left column: Negative average log-likelihood of the observed data marginalized over the model parameters  $\theta$ , i.e., the resampling weight for ModelSMC (Eq. 5). Right column: Negative average log-likelihood of the observed data given the parameter estimate  $\hat{\theta}$  (Eq. E-40)